

**EFFECT OF VELOCITY ON TRACTIVE
PERFORMANCE OF TRACTOR TIRES**

By

JOSEPH GARLAND GREENLEE

Bachelor of Science in Agricultural Engineering

Oklahoma State University

Stillwater, Oklahoma

1985

**Submitted to the Faculty of the
Graduate College of the
Oklahoma State University
in partial fulfillment of
the requirements for
the degree of
MASTER OF SCIENCE
December, 1986**

Thesis
1986
G814e
cop 2



EFFECT OF VELOCITY ON TRACTIVE
PERFORMANCE OF TRACTOR TIRES

Thesis Approved:

James D. Summers

Thesis Adviser

John B. Solie

Richard W. Whitney

Norman N. Durham

Dean of the Graduate College

1263848

PREFACE

Tests were designed by the use of dimensional analysis to determine the effect that velocity has on tractive effort. A mathematical model was then developed to predict tractive effort as a function of wheel slip, soil strength indicator, tire parameters and velocity. The model appears to be adequate for many design problems in the agricultural and industrial equipment industries.

I wish to express my sincere gratitude to all the people who assisted me in this work. In particular, I am especially indebted to my major advisor, Dr. Jim Summers for his intelligent guidance, unique comments and help in the field as well as the office. Special thanks are also due to the staff at the Agricultural Engineering labs for their help in completing the project.

Finally, I would like to express my appreciation to my wife, Tonya, my son, Jonathan and both sets of my parents, Mr. and Mrs. Joe Greenlee and Mr. and Mrs. JD Leach. Without their encouragement the work would never have been completed.

TABLE OF CONTENTS

Chapter	Page
I. INTRODUCTION	1
Objectives.	1
II. LITERATURE REVIEW.	3
III. PROCEDURE.	7
Dimensional Analysis Approach	7
Plot Layout	11
Field Preparation	11
Cone Penetrometer	14
Tire Testing Apparatus.	14
Test Tires.	21
Rolling Radius.	21
Tire Testing Procedure.	22
IV. RESULTS AND DISCUSSION	25
Rolling Resistance.	25
Gross Pull.	28
V. SUMMARY AND CONCLUSIONS.	60
VI. SUGGESTIONS FOR FURTHER RESEARCH	63
REFERENCES CITED.	65
APPENDIX A - BASIC PROGRAM FOR TIRE TEST MACHINE.	67
APPENDIX B - MACHINE LANGUAGE SUBROUTINE FOR DATA COLLECTION	74
APPENDIX C - COMPUTER MEMORY MAP FOR TIRE TEST MACHINE.	80
APPENDIX D - ROLLING RADIUS DATA.	81
APPENDIX E - PROGRAM TO INPUT TIRE TEST DATA TO IBM-PC	82
APPENDIX F - PROGRAM TO INPUT CONE INDEX DATA TO IBM-PC	84

Chapter	Page
APPENDIX G - TIRE TEST AND CONE INDEX DATA.	86
APPENDIX H - π TERM GENERATION PROGRAM.	91
APPENDIX I - π TERM DATA.	92
APPENDIX J - DATA FOR VALIDATION OF PREDICTION EQUATION	96

LIST OF TABLES

Table	Page
I. Pertinent Quantities and Symbols.	7
II. Dimension Matrix.	8
III. π Terms	9
IV. π Term Matrix	10
V. Configuration Identification.	12
VI. Analysis of Variance With π_{4b}	29
VII. Analysis of Variance With π_{4a}	29
VIII. Points Used To Fit Modified Witch of Agnesi Curve	48

LIST OF FIGURES

Figure	Page
1. Field Layout	13
2. Cone Penetrometer.	15
3. Microcomputer Used As Data Logger.	15
4. Tire Test Machine.	16
5. Load Cells Used to Indicate Pull and Change in Vertical Load on Tire.	16
6. Hydrostatic Transmission Used to Power Test Tire .	18
7. Side View of Chain Drive	18
8. Axle Speed Hall Effect Switch.	19
9. Fifth Wheel.	19
10. Ballast Rack With Lead Bars.	20
11. Hydraulic Motor to Develop Restraining Force Against Test Tire.	20
12. Selection of Tires Used in Test.	21
13. Load versus Rolling Radius for Tires Used.	23
14. Tire Test Machine in Operation	24
15. Predicted versus Measured Rolling Resistance . . .	27
16. K versus Actual Velocity	33
17. K versus Actual Velocity Squared	34
18. K versus Theoretical Velocity.	35
19. K versus Theoretical Velocity Squared.	36

Figure	Page
20. Predicted Gross π_1 versus Measured Gross π_1 for 16.9-30 Tire Only	38
21. Predicted Gross π_1 versus Measured Gross π_1 for All Five Tires.	39
22. K versus π_5	40
23. A versus π_5	42
24. Predicted Gross π_1 versus Measured Gross π_1	44
25. Predicted Gross π_1 versus Measured Gross π_1 With Slope Corrected.	45
26. K versus Theoretical π_4 With Modified Witch Of Agnesi Curve	49
27. A versus π_5	51
28. Predicted Net π_1 versus Measured Net π_1	53
29. Predicted Net π_1 versus Measured Net π_1 for Firestone 16.5L-16.1, I-3 Traction Implement Tire	54
30. π_1 versus π_2	55
31. π_1 versus π_3	56
32. π_1 versus Theoretical Velocity	57
33. π_1 versus π_5	59

CHAPTER I

INTRODUCTION

To accurately simulate vehicle performance, all elements pertinent to the vehicle system must be mathematically defined. One of these elements is tractive force. For agricultural tractors, tractive force is developed at the soil-tire interface. Forces developed at this interface can not be defined explicitly, primarily due to the complex dynamic stress-strain relationship of the soil. Another approach to predict tractive force is to develop an empirical model from actual field test data of tires on soils with several hardnesses.

As pointed out by Yong et al. (1984), tractive force is a function of both cohesive soil reactions, which are strain rate dependent, and frictional soil reactions. For strain rate to be a factor, the soil is presumed to have plastic strain characteristics. Since the strain rate of the soil-tire interface is a function of both tire slip and tire peripheral velocity, a function of velocity should be included in the traction prediction equation.

Objectives

The overall objective of this research was to determine

the effect of velocity on pull developed by a lugged, agricultural tire in field conditions. This was accomplished by completing the following specific objectives:

1. Determine parameters affecting tractive performance of a lugged tractor tire in field conditions by use of dimensional analysis techniques.
2. Develop a tractive force prediction equation for lugged tractor tires in field conditions.

CHAPTER II

LITERATURE REVIEW

Wisner and Luth (1974), developed the following equation using dimensional analysis techniques to predict pull of off-road vehicles:

$$\frac{P}{W} = .75(1 - e^{-0.3CnS}) - \left(\frac{1.2}{Cn} + 0.04\right) \quad (1)$$

where:

$$\begin{aligned} \frac{P}{W} &= \text{Pull to weight ratio} \\ Cn &= \text{Wheel numeric} = \frac{CIbd}{W} \\ CI &= \text{Cone index value} \\ b &= \text{Tire section width} \\ d &= \text{Tire diameter} \\ W &= \text{Dynamic load on tire} \\ S &= \text{Wheel slip} \end{aligned}$$

Tires tested were a variety of small (diameters less than 150 mm), smooth tires (with the exception of one lugged tire) at speeds lower than typical field speeds (less than 2.25 km/h). Since these tests were performed in a soil bin, field speeds were unattainable. In this study, it was assumed that velocity has little effect on tractive performance.

Dwyer et al. (1976) published a handbook for agricultural tire performance. This handbook lists the tractive coefficients for different tractor tires for a variety of surface conditions and two wheel slips. Bloome

et al. (1983) compared data from this handbook to the Wismer and Luth prediction equation. This comparison illustrated that the Wismer and Luth equation failed to predict the data from Dwyer et al. (1976) satisfactorily. This confirms that the prediction equation is not adequate for agricultural tires operating in field conditions.

One variable needed in tractive force calculations is the soil strength or soil cone index. Clark (1985) examined the sensitivity of predicted tractive force using cone index values averaged over different depths. His results indicated that for bare soils, the cone index value should be averaged over a depth range of 0 to 15 cm.

Another important factor in tractive performance is wheel slip. Brixius and Wismer (1978) studied the role of slip in traction. The ratio of pull to dynamic load increased with slip to approximately 30%, then became asymptotic as slip continued to increase.

To calculate wheel slip, the angular velocity and effective rolling radius along with translational velocity are needed. The effective rolling radius of a tire is a measure of the number of revolutions made by the tire as it travels a given distance. Charles and Schuring (1984) developed an empirical equation to predict effective rolling radius. This equation calculates rolling radius as a function of the unloaded tire radius, loaded tire radius, and a dimensionless factor. This equation will predict rolling radius of the tire on varying surface conditions.

Burt and Lyne (1983) studied the effect of velocity on tractive performance. Within the velocity range of 0.1 m/s to 0.6 m/s, there was no effect of forward velocity on net traction for constant slip and dynamic load. The upper end of this range is about one-fourth of the operating speeds of today's agricultural equipment.

Gee-Clough et al. (1977) studied the effect of velocity on tractive performance with tractors in the field conditions. These tests showed increased pull with increased velocity. Since these tests were performed over two years, environmental effects caused wide deviations in the data.

Bekker (1969) stated the effect of strain rate on soil shear strength can be considered non-existent in the range of strain rates typical for off-road traction devices. This appears contradictory with information from Gee-Clough et al. (1977) and Yong et al. (1984).

McAllister et al. (1976) studied the effect of aspect ratio on tractive performance of agricultural tires. The results indicate the only advantage of using a tire with a low aspect ratio is the ability to carry a given load at a lower tire pressure.

Keed et al. (1964) studied the effect of tire diameter on performance. They found that a larger diameter tire can be loaded and operated so as to give a significant increase in pull over a smaller diameter tire, however, the differences come from several factors and not diameter

alone. The most important factor affecting pull of a tire is the soil condition.

CHAPTER III

PROCEDURE

Dimensional Analysis Approach

Through the use of dimensional analysis, an equation can be developed for traction prediction accounting for velocity. This first requires a list of the pertinent quantities. The pertinent quantities considered in this research are listed in Table I.

TABLE I
PERTINENT QUANTITIES AND SYMBOLS

<u>Symbol</u>	<u>Parameter</u>	<u>Dimensions</u>
P	Pull	F
W	Vertical dynamic load	F
CI	Cone index	FL ⁻²
b	Tire width	L
d	Tire diameter	L
V	Velocity*	LT ⁻¹
S	Wheel slip	--
g	Gravitational constant	LT ⁻²

*Velocity could either be actual (translational) velocity or theoretical (peripheral) velocity.

According to Murphy (1950), Buckingham's π theorem states:

"... the number of dimensionless and independent quantities required to express a relationship among the variables in any phenomenon is equal to the number of quantities involved, minus the number of dimensions in which those quantities may be measured."

The dimension matrix used to determine the number of dimensionless π terms required is listed in Table II.

TABLE II
DIMENSION MATRIX

	P	W	CI	b	d	V	S	g
F	1	1	1	0	0	0	0	0
L	0	0	-2	1	1	1	0	1
T	0	0	0	0	0	-1	0	-1

Rank of matrix = 3

Number of parameters = 8

Number of terms needed $(8-3) = 5$

This indicates that 5 terms from the pertinent quantities can be developed.

To determine the π terms, Murphy (1950) states:

"... the only restrictions placed upon π terms is that they be dimensionless and independent."

By referring to work reported in literature, a set of π terms that appears to describe all the pertinent quantities was then selected. The π terms selected for this research

are given in Table III. Note the four options for the velocity factor.

The way to check the π terms for independence is to compare the number of π terms to the rank of the π term matrix as illustrated in Table IV. Since the rank of the π term matrix (Table IV) was equal to the number of π terms, the terms are all independent.

TABLE III
 π TERMS

π term	Description	
$\pi_1 = \frac{P}{W}$	Tractive coefficient	(2)
$\pi_2 = \frac{CIbd}{W}$	Wheel numeric	(3)
$\pi_3 = S$	Wheel slip	(4)
$\pi_{4b} = \frac{v^2}{gb}$	Velocity* coefficient	(5)
$\pi_{4d} = \frac{v^2}{gd}$	Velocity coefficient	(6)
$\pi_5 = \frac{b}{d}$	Aspect ratio	(7)

*Velocity could either be actual (translational) velocity or theoretical (peripheral) velocity.

The prediction equation will have the form of;

$$\frac{P}{W} = f\left(\frac{CIbd}{W}, S, \frac{V^2}{gb}, \frac{b}{d}\right) \quad (8)$$

or

$$\frac{P}{W} = f\left(\frac{CIbd}{W}, S, \frac{V^2}{gd}, \frac{b}{d}\right) \quad (9)$$

TABLE IV

π TERM MATRIX

	P	W	CI	b	d	V	S	g
π_1	1	-1	0	0	0	0	0	0
π_2	0	-1	1	1	1	0	0	0
π_3	0	0	0	0	0	0	1	0
π_4	0	0	0	-1	0	2	0	-1
π_5	0	0	0	1	-1	0	0	0

By inspection, it can be seen that each π term can be varied by altering one variable in the π term at a time.

The procedure for doing this was:

- a) π_1 was the dependent variable.
- b) π_2 was varied by:
 - 1) changing soil cone index.
 - 2) changing tire section width.
 - 3) changing tire diameter.
 - 4) changing vertical load on tire.
- c) π_3 was varied by changing wheel slip.
- d) π_4 was varied by changing the theoretical wheel velocity.
- e) π_5 was varied by changing tires sizes.

Plot Layout

To determine the effects the π terms have on tractive performance of tractor tires, test procedures require varying the five π terms individually. A strip plot design was chosen to get three cone index levels on all tests. The other variables used were five tire sizes, four velocities, four wheel slips and four vertical wheel loads. This gave an experimental plot design with 14 treatments per replication as shown in Table 5.

This design was replicated four times for the pull test and one test measuring rolling resistance. This required a field 72 m wide and 210 m long. The field used had a sandy-loam type soil and was located at the South Central Research Station in Chickasha, OK.

A four character code was used to identify individual test runs. The first digit ranged from 1 to 3 and indicated cone index level. The second digit ranged from 1 to 5 with 1 to 4 indicating pull test replication and 5 indicating rolling resistance test. The last two letters were the test configuration code illustrated in Table 5.

Field Preparation

To achieve the correct soil texture for compacting the plots, the field was tilled with a chisel plow and tandem disc. The field was then flagged to form a grid pattern to the dimensions shown in Figure 1.

To achieve the three cone index ranges, a 26.7 kN sheep

TABLE V
CONFIGURATION IDENTIFICATION

EXPERIMENT DESIGN

Config.	bd	W	CI	S	V
AA	1	1	1, 2, 3	1	1
BA	2	1	"	1	1
CA	3	1	"	1	1
DA	4	1	"	1	1
EA	5	1	"	1	1
FA	1	2	"	1	1
GA	1	3	"	1	1
HA	1	4	"	1	1
AB	1	1	"	2	1
AC	1	1	"	3	1
AD	1	1	"	4	1
AE	1	1	"	1	2
AF	1	1	"	1	3
AG	1	1	"	1	4

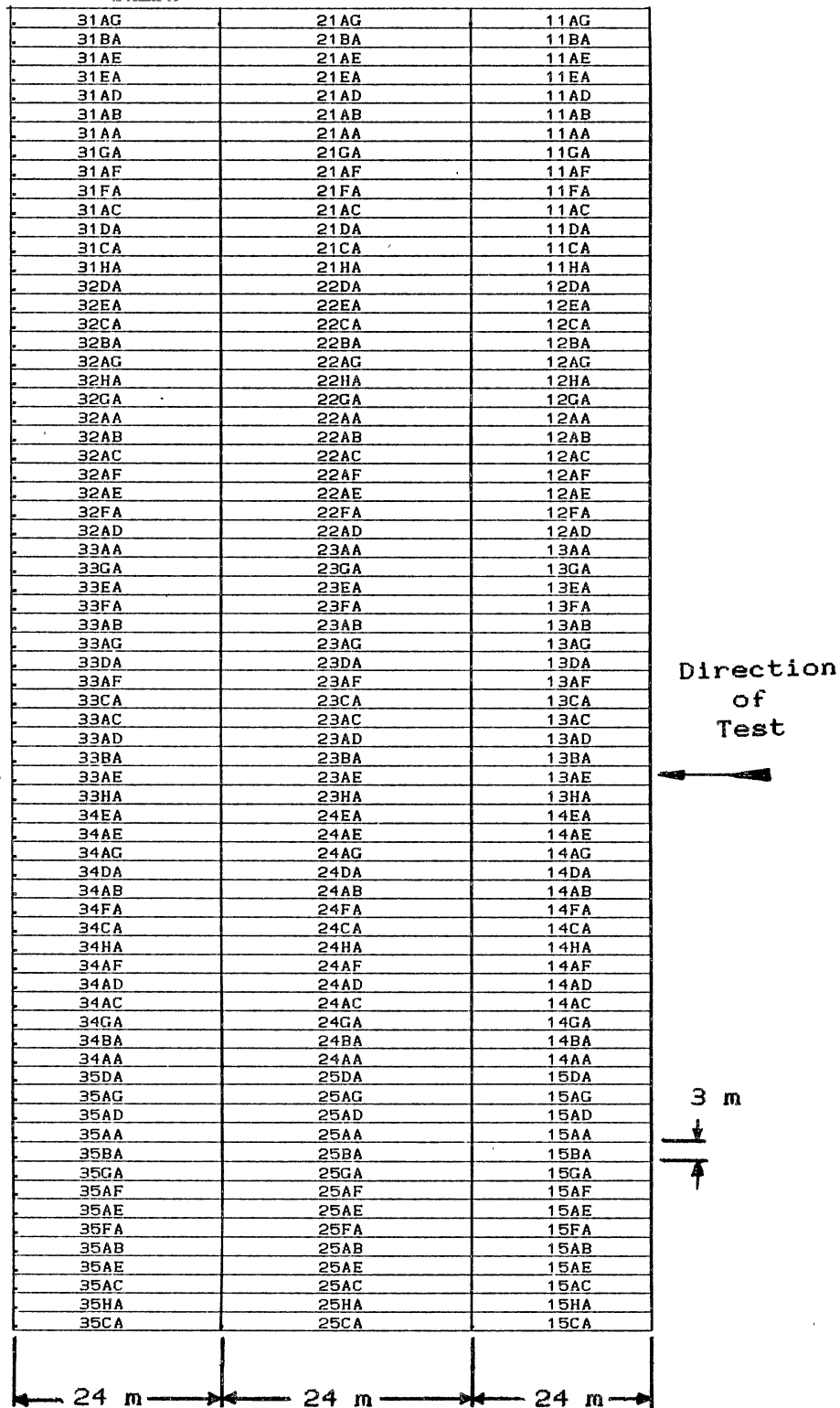


Figure 1. Field Layout

foot roller and a 97.9 kN Gallion pneumatic tire roller were used. The first cone index level was left in the tilled condition to give an average cone index level of 370 kPa. The second cone index strip was rolled 3 times with both rollers, giving an average cone index value of 508 kPa. The third strip was rolled until cone penetrometer readings reached a maximum indicating the soil stopped compacting. This level had an average cone index level of about 607 kPa.

Cone Penetrometer. Before each tire test was performed, cone penetrometer readings were taken. The cone index value was obtained from an average of six probings taken through the length of the plot. The value obtained from each individual probing was an average of the top 15 cm of soil. The penetrometer used was developed by Riethmuller, et al. (1982) shown in Figure 2 and equipped with an upgraded AIM 65 microcomputer based data logger (Summers et al., 1986) shown in Figure 3. The data logger measured the output voltage of the force transducer, which sensed the force on the probe. The output data was an average cone index value for the top 15 cm of soil.

Tire Testing Apparatus. A single-tire test apparatus was designed and built using a R6510 Ditch Witch machine as the power source. The digger bar was replaced by a frame to hold the test tire as shown in Figure 4. Three load cells were placed between the frame and digger drive (shown in Figure 5). These load cells measured pull and change in

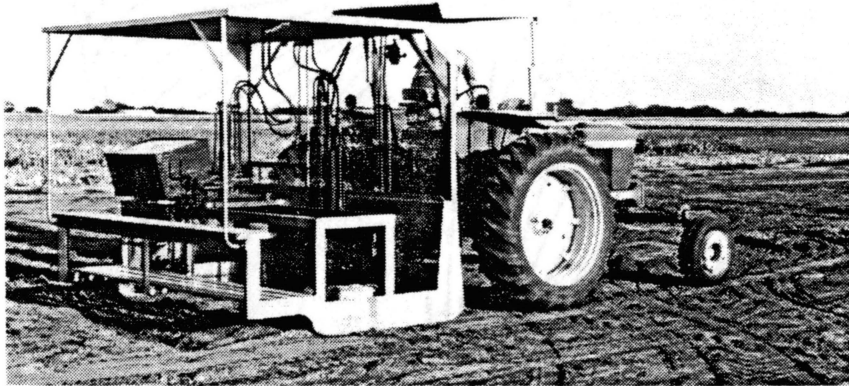


Figure 2. Cone Penetrometer

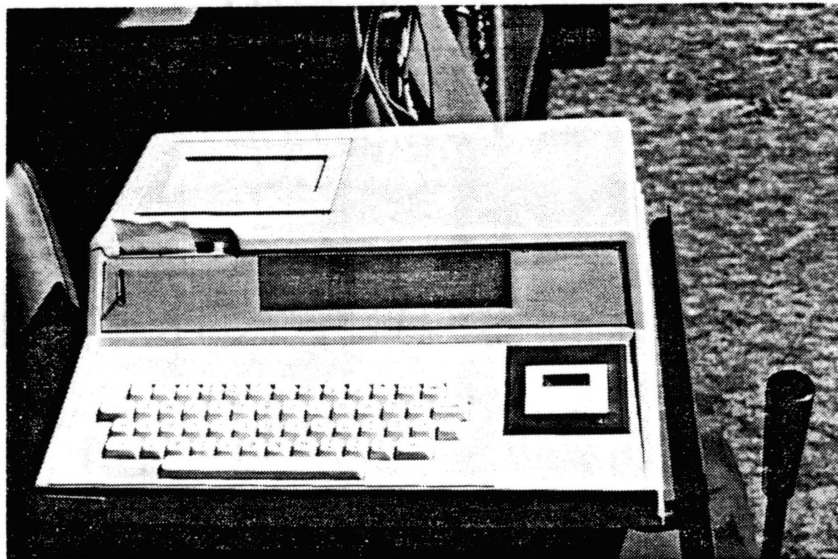


Figure 3. Microcomputer used As Data
Logger

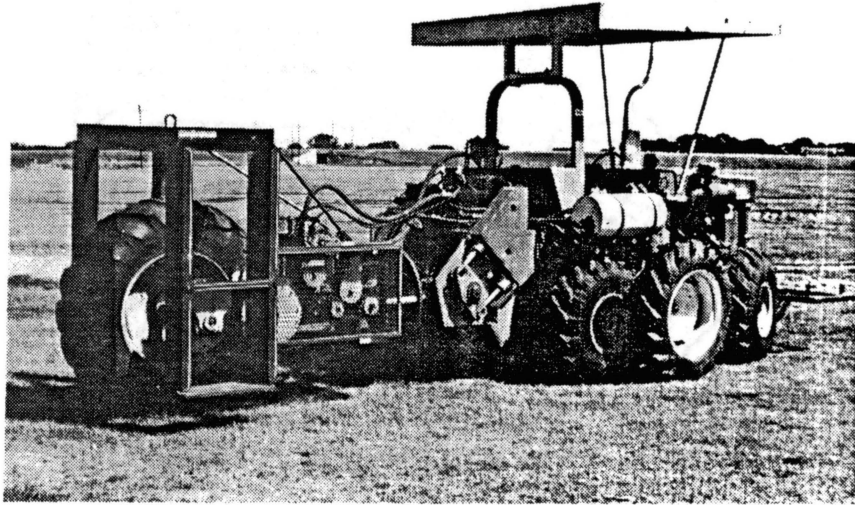


Figure 4. Tire Test Machine

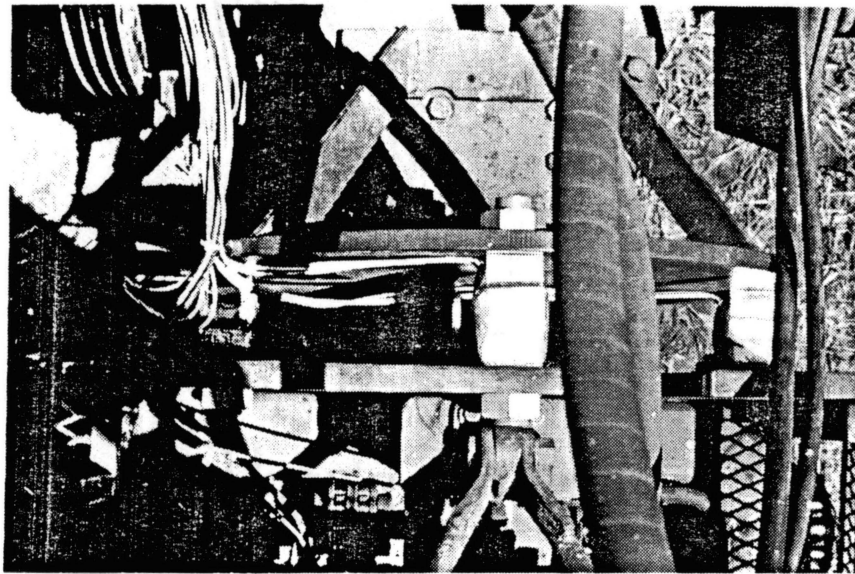


Figure 5. Load Cells (top view) Used to Indicate Pull and Change in Vertical Load on Test Tire

vertical load that the test frame exerted on the R6510 during testing. Dynamic load was then calculated from static load and change in vertical load measured by the load cells.

Power to the test tire was provided by a hydrostatic transmission driven by the digger drive (Fig. 6). Power was then conveyed through a series of chain drives (Fig. 7). The chain drives were used for a positive speed reduction of 28.125. A hall effect switch (Fig. 8) was used to determine the axle speed. A fifth wheel mounted on the R6510 was used to measure the actual velocity (Fig. 9). Wheel slip was calculated from these two variables.

Static load was added to the test tire by adding lead bars to both sides of the rack suspended by bearings from the test tire axle (Fig. 10). This ensured all of the load added was carried by the test tire. Transducers were monitored with the data logger. Data was collected using the programs listed in Appendices A and B and stored in memory locations listed in Appendix C. Three sets of data were collected on command from the operator, then displayed, printed to paper and stored on cassette tape. All reduction of raw data was done on-board and only data in engineering units were stored.

Restraining load for the test tire to develop various levels of pull was provided by the R6510 drive train. A hydraulic motor (Fig. 11) was connected to the drive shaft between the two differentials. As more restraining load

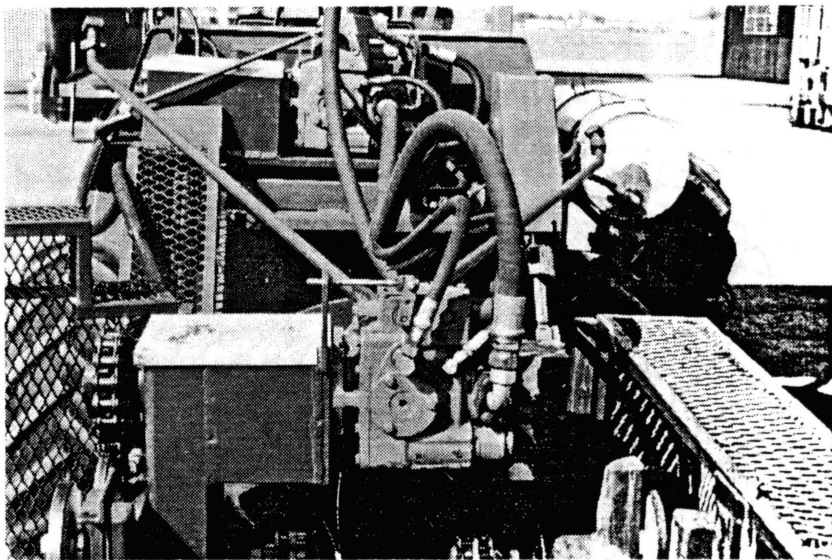


Figure 6. Hydrostatic Transmission Used to Power Test Tire

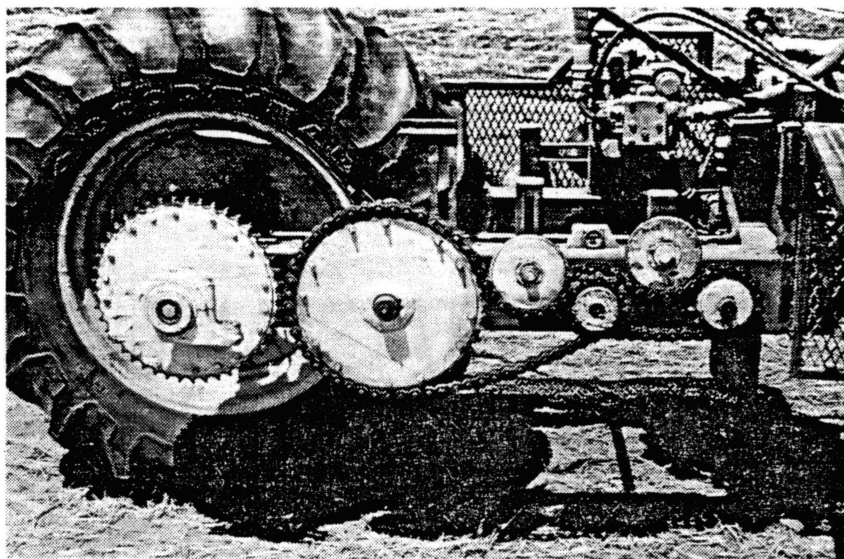


Figure 7. Side View of Chain Drive

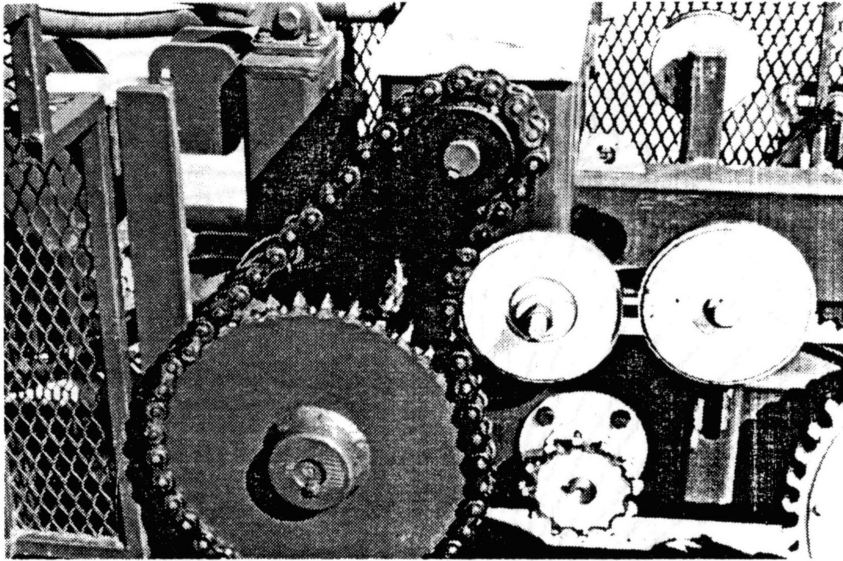


Figure 8. Axle Speed Hall Effect Switch

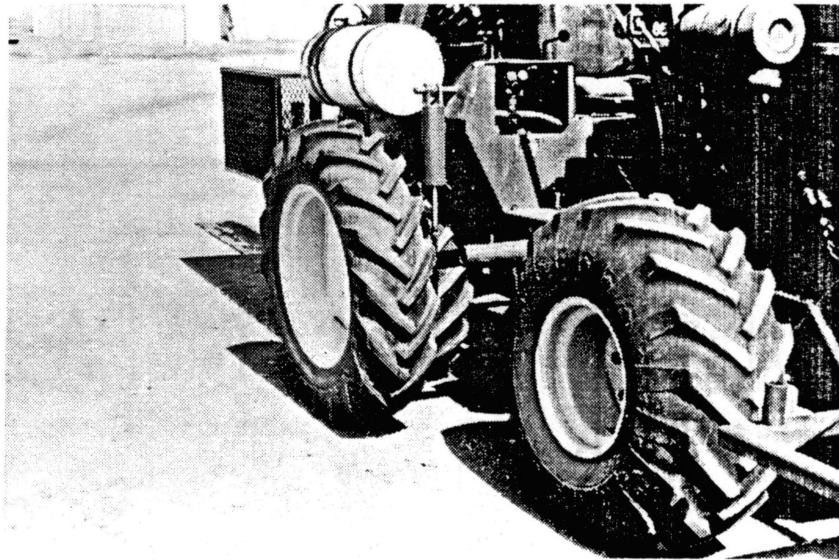


Figure 9. Fifth Wheel

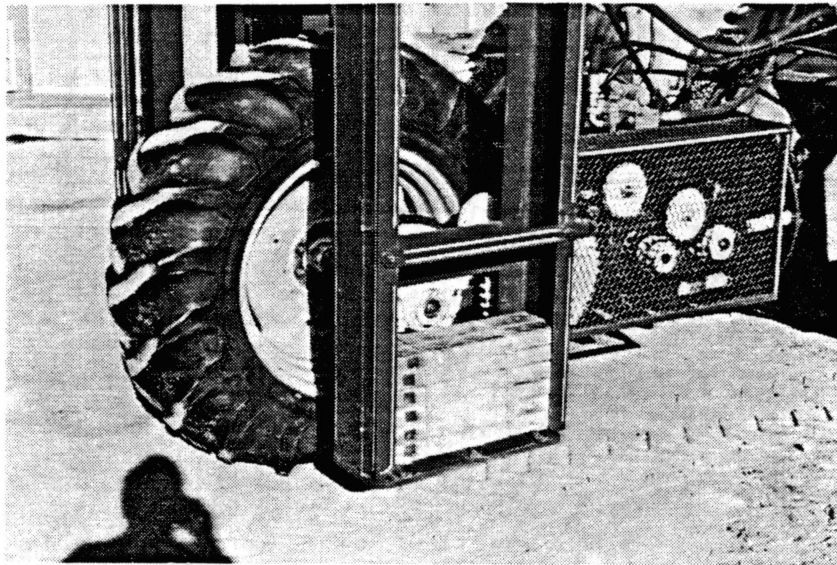


Figure 10. Ballast Rack with Lead Bars

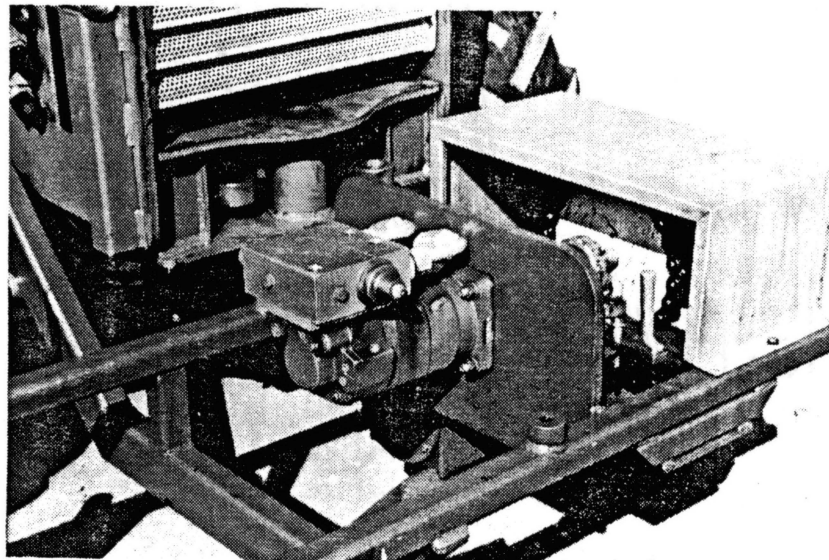


Figure 11. Hydraulic Motor to Develop Restraining Force Against Test Tire

was desired, the hydraulic motor was slowed causing the test tire to pull against the R6510.

Test Tires. Five R-1 traction tires were chosen to be used in this test. These tires, shown in Figure 12, are from left to right, 8.3-24, 11.2-38, 15.5-38, 16.9-30 and 18.4R38. The second and third tires were chosen to get a comparison of section width. The other tires were chosen to vary the diameter.

Rolling Radius. The rolling radius for each of the five tires with the four specified loads was needed for computations during data acquisition. This was measured by mounting each of the tires in the tire test machine and



Figure 12. Selection of Tires Used
in Test

measuring the distance required to roll the tire either 15 or 20 revolutions (depending on the tire diameter) on a firm, flat surface. This data is listed in Appendix D and a graph of rolling radius versus wheel load is given in Figure 13.

Tire Testing Procedure. After determining the cone index for a plot, the tire test machine was oriented in such a way that the test tire would pull the machine in a reverse direction (from right to left in Fig. 14). The machine required two operators. The first operator controlled the speed and slip of the test tire while the other operator steered the machine and operated the computer. Since the strip plot design was used, the machine was not stopped until all three cone index levels were tested. This made it faster and easier to replicate the velocity and slip level used on that particular test. The rolling resistance test was performed in the same manner except the drive chains to the axle was removed to allow the test tire to roll freely.

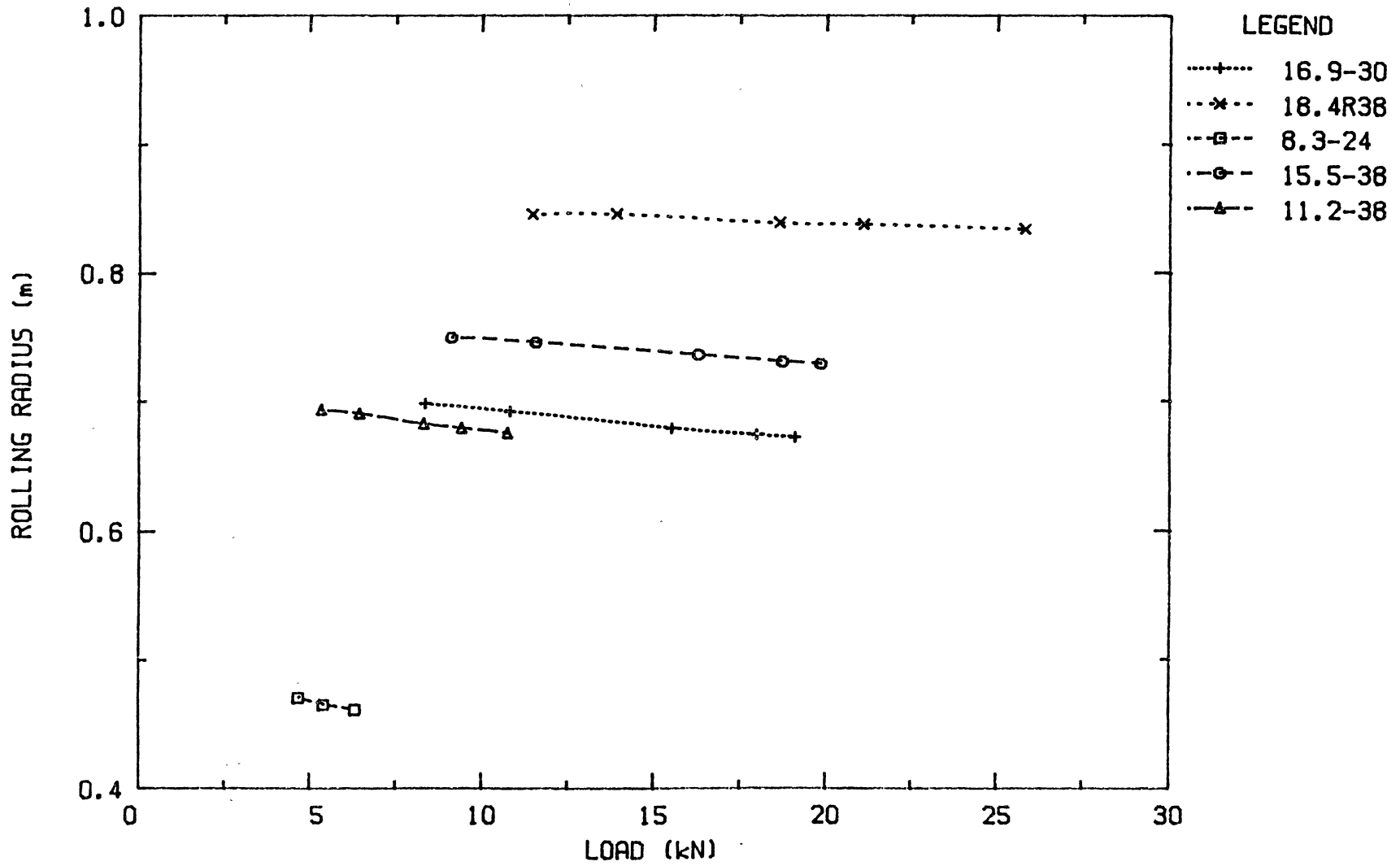


Figure 13. Load versus Rolling Radius for tires used

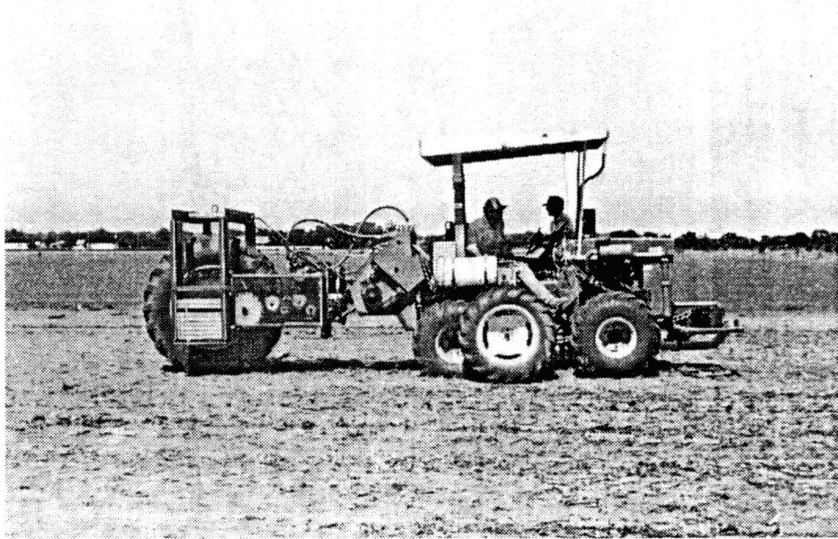


Figure 14. Tire Test Machine in Operation

CHAPTER IV

RESULTS AND DISCUSSION

Tire test data collected during field tests were input into the IBM-PC with programs listed in Appendices E and F and is listed in Appendix G. The program listed in Appendix H was then implemented to transform the data into the terms shown in Appendix I. The soil was a McClain silt loam with the taxonomic description of Fine, Mixed, Thermic Pachic Argiustoll. moisture content of 15.6 % (d.b.) was measured from thirteen randomly selected soil samples taken in the test field. Moisture content, however, was not treated as a pertinent quantity.

Rolling Resistance

The rolling resistance data (fifth replication) was separated from the data to be analyzed first. For this replication, π_1 represents the towed force-to-dynamic load ratio. Since wheel slip is not a factor and velocity has little affect on rolling resistance (Steiner and Sohne, 1979), the only π terms that affect rolling resistance are π_2 and π_5 given in Equations (3) and (7) respectively.

The expression for rolling resistance was obtained by first plotting π_1 , (TF/W), against π_2 with π_5 held at a

constant value to find an expression for π_2 . The form of the expression was:

$$\pi_1 = a_0 + \frac{a_1}{\pi_2} \quad (10)$$

This form is the same form used by Wismer and Luth (1974). Then π_1 was plotted against π_5 with π_2 held constant. The best fit of these points was a simple linear regression having the form:

$$\pi_1 = a_2 + a_3 \pi_5 \quad (11)$$

A similitude approach was used to combine the two expressions. Since the two expressions plot linearly on arithmetic paper, they can be combined by addition resulting in:

$$\frac{TF}{W} = a_0 + \frac{a_1}{\pi_2} + a_2 \pi_5 \quad (12)$$

A multiple regression software package was then used to determine the equation that best fit the rolling resistance data. The constants found were:

$$\begin{aligned} a_0 &= 0.229 \\ a_1 &= 0.234 \\ a_2 &= -0.704 \end{aligned}$$

with a coefficient of determination (R^2) of 0.719.

A plot of the predicted rolling resistance against the measured rolling resistance is shown in Figure 15.

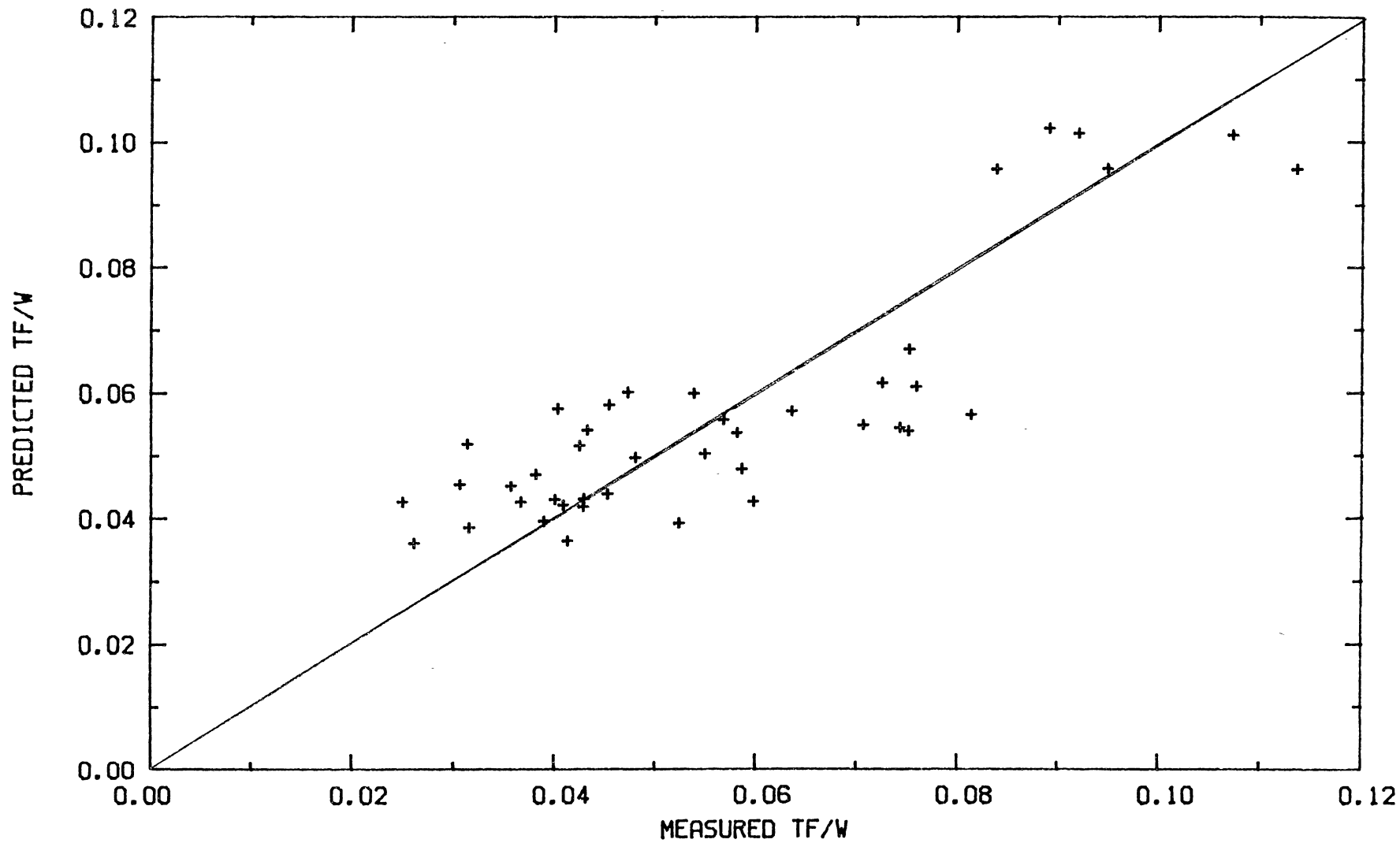


Figure 15. Predicted versus Measured Rolling Resistance

Gross Pull

Since the coefficient of determination is not valid for nonlinear regression analysis (Draper and Smith, 1966), another means of comparing the quality of fit is needed. One method is to plot predicted data against measured data. Linear regression can be used to determine the best fit line through the data. An ideal fit would be:

1. $R^2 = 1$.
2. The slope of the regressed line be one.
3. The intercept of regressed line be zero.

An analysis of variance was performed on the pull data using π_{4b} and π_{4d} to determine the interaction of variables. Tables VI and VII show the analysis of variance tables using π_{4b} and π_{4d} respectively. From Table V, the significant variables are π_2 , π_3 , π_{4b} and π_5 . The interaction of π_2 , π_3 and π_{4b} is marginally significant. This means that the π terms are not independent of one another and a similitude approach would be impossible. From Table VI, it can be seen that none of the π terms have any interaction. This means the product or quotient of any two π terms will have a negligible effect on the model. During testing, the operators could not operate at particular variable values such as the prescribed velocity and wheel slip. Due to this, the similitude approach used in the rolling resistance analysis was not as effective. For this reason, the nonlinear

TABLE VI
ANALYSIS OF VARIANCE WITH π_{4b}

Source	df	Sum of Squares	F Value	PR > F
π_2	5	0.07688928	8.00	0.0001
π_3	16	0.09980424	3.24	0.0024
$\pi_2 \times \pi_3$	4	0.00640443	0.83	0.5147
π_{4b}	8	0.06903995	4.49	0.0011
$\pi_2 \times \pi_{4b}$	3	0.00127436	0.22	0.8811
$\pi_3 \times \pi_{4b}$	6	0.00703282	0.61	0.7207
$\pi_2 \times \pi_3 \times \pi_{4b}$	1	0.00419991	2.18	0.1495
π_5	1	0.00650142	3.38	0.0755
$\pi_2 \times \pi_5$	0	0.0	--	--
$\pi_3 \times \pi_5$	0	0.0	--	--
$\pi_{4b} \times \pi_5$	0	0.0	--	--

TABLE VII
ANALYSIS OF VARIANCE WITH π_{4d}

Source	df	Sum of Squares	F Value	PR > F
π_2	5	0.05534596	5.92	0.0006
π_3	16	0.10115447	3.38	0.0016
$\pi_2 \times \pi_3$	9	0.01075874	0.64	0.7554
π_{4d}	8	0.07002641	4.68	0.0007
$\pi_2 \times \pi_{4d}$	4	0.00253660	0.34	0.8496
$\pi_3 \times \pi_{4d}$	7	0.01312686	1.00	0.4478
$\pi_2 \times \pi_3 \times \pi_{4d}$	0	0.00000000	--	--
π_5	3	0.02103724	3.75	0.0205
$\pi_2 \times \pi_5$	0	0.0	--	--
$\pi_3 \times \pi_5$	0	0.0	--	--
$\pi_{4d} \times \pi_5$	0	0.0	--	--

regression (NLIN) in the Statistical Analysis System (SAS, 1982) was used.

A series of models were developed and tested with NLIN. The models were based on the assumptions that slip (π_2) and wheel numeric (π_3) affect π_1 asymptotically. Zero wheel slip is referenced to the towed tire. π_{4b} or π_{4a} and π_5 were included in these models additively or multiplicatively in several mathematical forms. Equations (13) through (17) list the different forms used.

$$\text{Linear} \quad \pi_1 = a_0 + a_1 \pi_x \quad (13)$$

$$\text{Inverse X\&Y} \quad \pi_1 = a_0 + \frac{a_1}{a_2 + \pi_x} \quad (14)$$

$$\text{Inverse X} \quad \pi_1 = a_0 + \frac{a_1}{\pi_x} \quad (15)$$

$$\text{Inverse Y} \quad \pi_1 = a_0 + \frac{1}{a_1 + a_2 \pi_x} \quad (16)$$

$$\text{Exponential} \quad \pi_1 = a_0 + a_1 e^{a_2 \pi_x} \quad (17)$$

where X indicates any π term or combination of π terms. Thirty five different models were tried using combinations of the five forms given in Equations (13) through (17). This was performed by starting with a base model believed to be close to the prediction equation according to the results of the analysis of variance. The best model was found by trying the π terms in the different forms and noting the change in the R^2 of the predicted data regressed to the measured data. When the effect of one π term on the model was defined, another π term was altered. This process was repeated until no more improvement was obtained

by altering the form of the π terms. This technique was used on several base models.

The best model found was:

$$\pi_1 \text{ (gross)} = A + B \pi_5 + \frac{C}{D + \pi_4} - Ee^{-F\pi_2} - Ge^{-H\pi_3} \quad (18)$$

where

A=1.11
B=-2.24
C=0.00798
D=0.0124
E=0.328
F=0.220
G=0.338
H=6.20

with a R^2 of 0.505.

Even though the above model has the highest R^2 of those used, this does not fit the boundary conditions required by a tractive effort model. One of the boundary conditions is that the gross pull should approach zero when the slip approaches zero. This fact alone indicates that this model fails to meet boundary conditions. The next best model had an R^2 of 0.260, which was too low for a complete model.

Another approach was then used to analyze the data. Data for only the 16.9-30 tire was regressed with NLIN to fit a form:

$$\pi_1 \text{ (gross)} = A(1 - e^{-K\pi_2\pi_3}) \quad (19)$$

with a R^2 of 0.471. This low R^2 was due to not taking into account all defined pertinent quantities of the system.

The coefficients obtained are:

A=0.481
K=1.35

The next variable to be incorporated in the equation was the velocity π term (π_{4d}). To achieve this, four plots were made to compare the coefficient K shown above to velocity where:

$$K = \frac{-\ln\left(1 - \frac{\pi_1}{A}\right)}{\pi_2 \pi_3} \quad (20)$$

and A was assumed to be 0.6 since the maximum gross pull-to-dynamic load ratio was slightly less than 0.6. This was assumed to prevent the argument of the natural log term from becoming undefined. Since only the 16.9-30 tire was used at this point, K was plotted against velocity and not π_{4d} . These plots are shown with their best fit regressions in Figures 16 through 19. The best velocity term was then found to be theoretical velocity squared. This allowed a new K value to be predicted for any square of theoretical velocity. After adjusting the constants so π_4 could be used instead of theoretical velocity squared, a prediction equation for predicting gross tractive effort for the 16.9-30 tire was:

$$\pi_1(\text{gross}) = 0.6 \left(1 - e^{\frac{-0.00236 \pi_2 \pi_3}{\pi_4}} \right) \quad (21)$$

When predicted π_1 was regressed on measured gross π_1 the result is:

$$\pi_1(\text{pred}) = .0300 + .886 \pi_1(\text{meas}) \quad (22)$$

with an R^2 of 0.402.

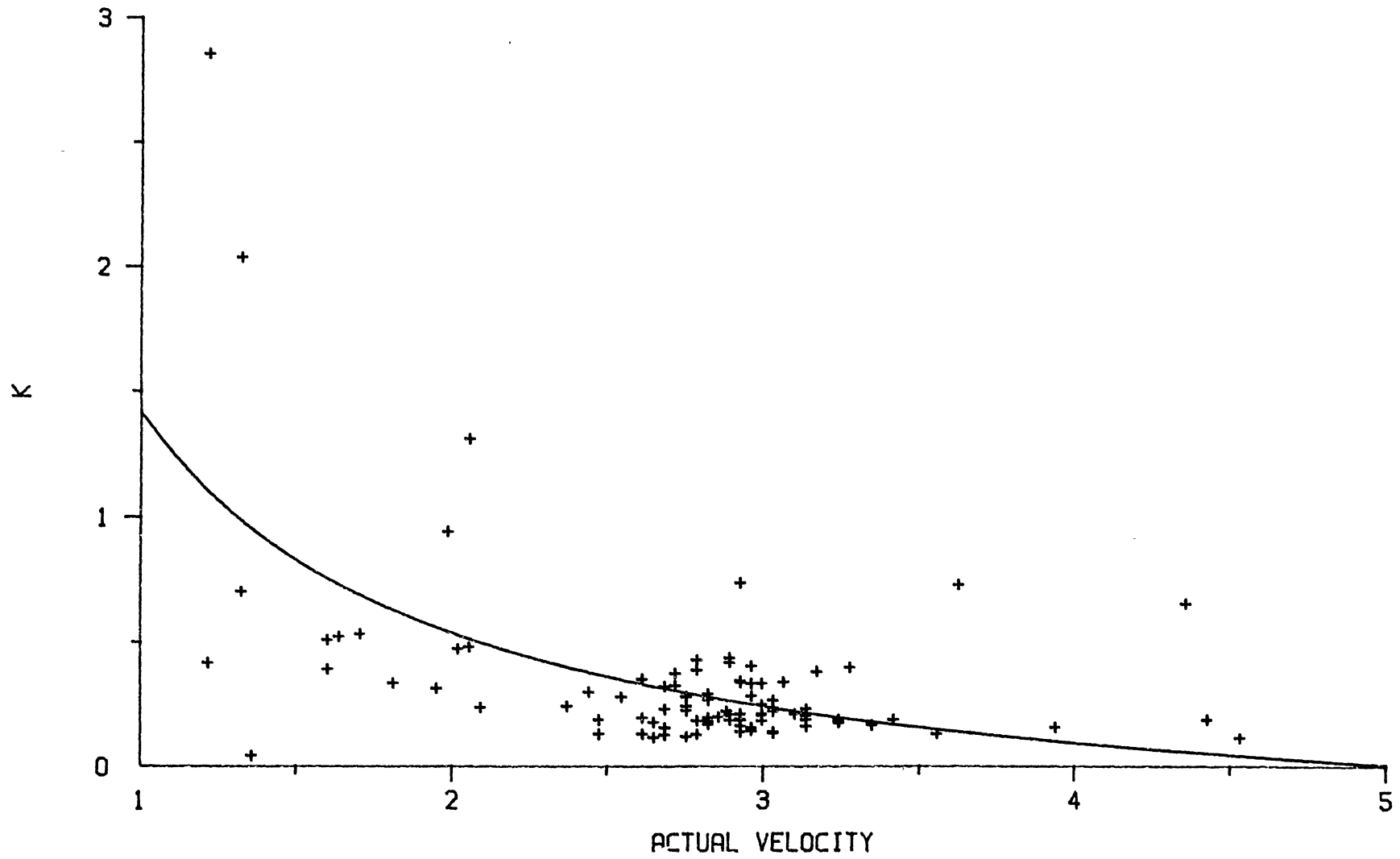


Figure 16. K versus Actual Velocity

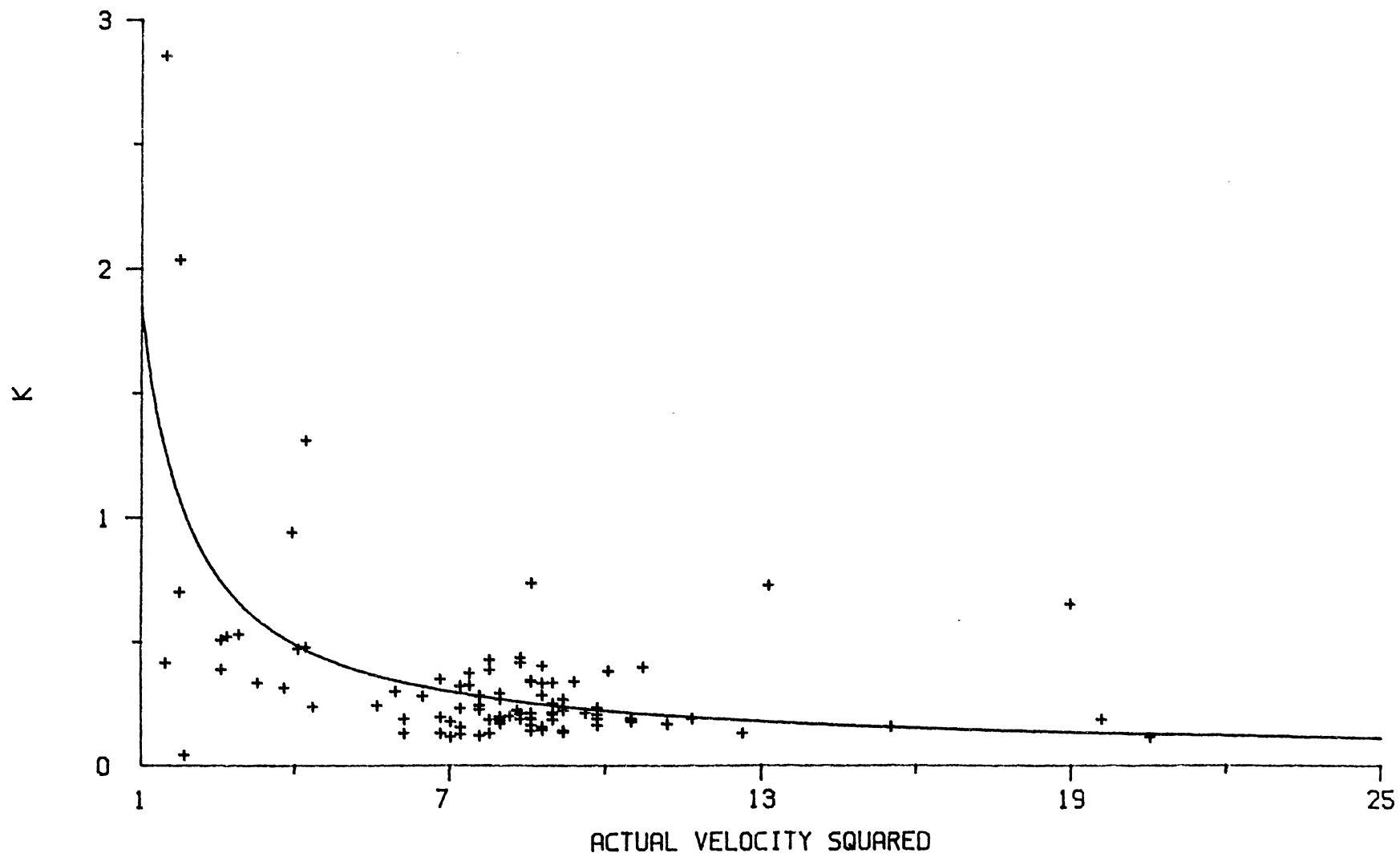


Figure 17. K versus Actual Velocity Squared

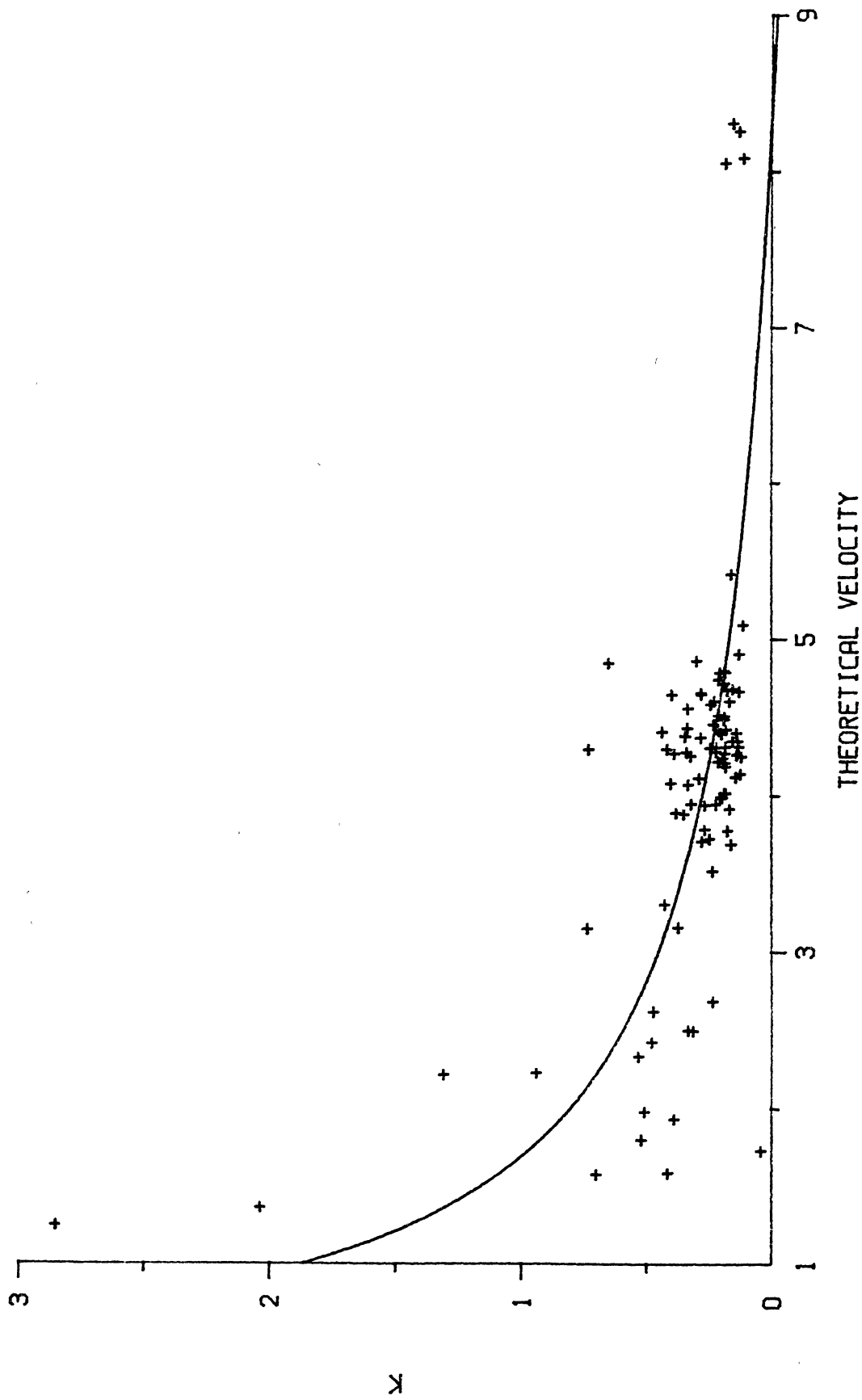


Figure 18. K versus Theoretical Velocity

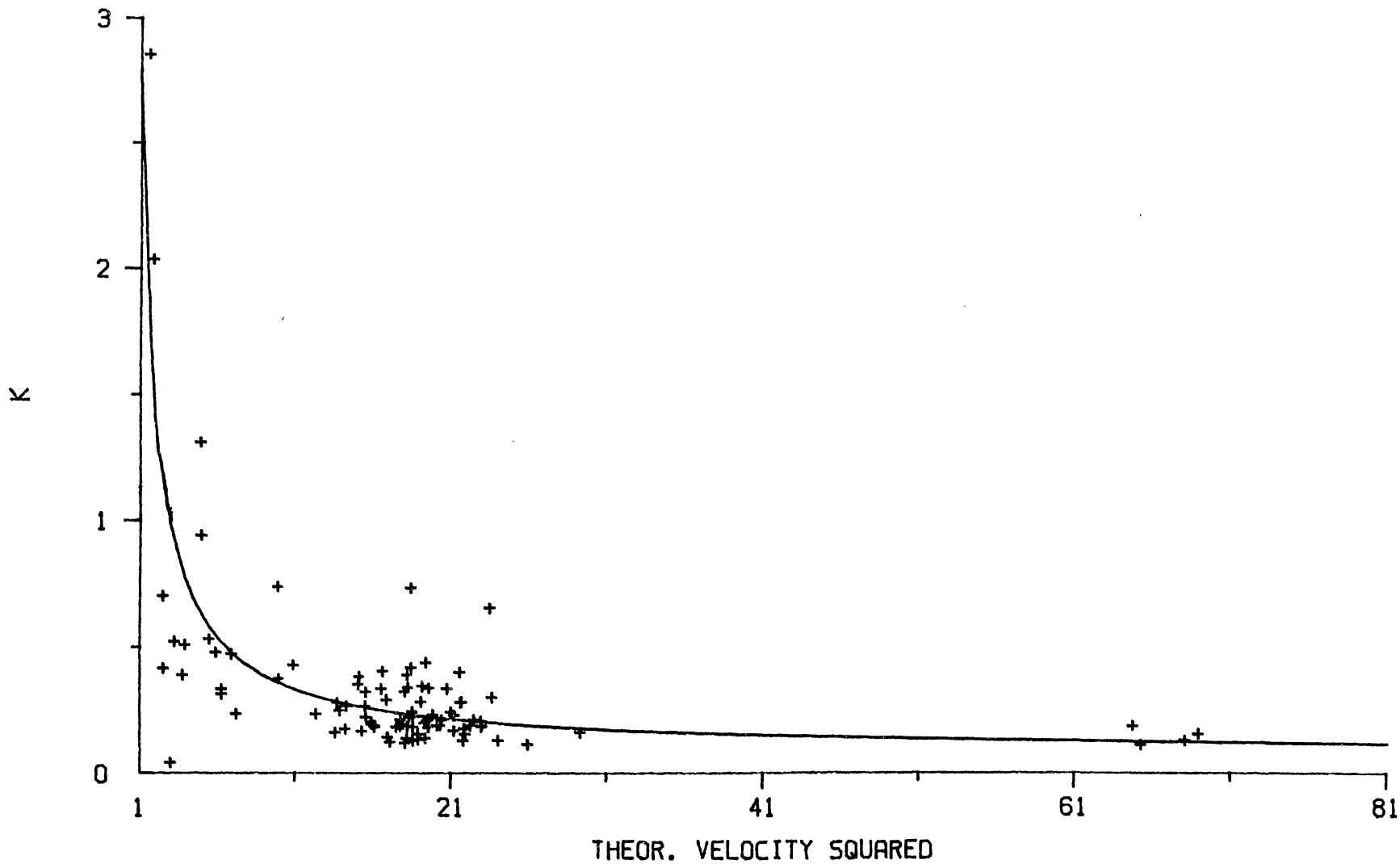


Figure 19. K versus Theoretical Velocity Squared

Since the intercept of the regressed equation is nearly zero, and the slope of the line is not quite one, this indicates that 0.6 was not the best estimate for A in Equation (20). Slight adjustments can be made to the asymptotic value A to make the slope of Equation (22) almost unity. This is done by dividing the prediction equation by the slope of the regressed line, giving a new prediction equation of:

$$\pi_1 (\text{gross}) = A \left(1 - e^{-\frac{K\pi_2\pi_3}{\pi_4}} \right) \quad (23)$$

where: A=0.677
 K=0.00236

with the same R^2 as obtained in Equation (22). This equation is plotted with the data in Figure 20.

The next step was to determine if the prediction equation was adequate to predict traction on all the tires tested. This was done by plotting predicted gross π_1 , Equation (23), against measured gross π_1 . This plot is shown in Figure 21. It can be seen from this graph that the tire parameters in π_2 , π_3 and π_4 are not enough to describe the performance of the tires. Another π term that describes the tire must be added to the gross pull prediction equation. The π term that best describes the tire is π_5 , the aspect ratio. To determine how π_5 interacts with the prediction equation, K was plotted against π_5 (Fig. 22) where:

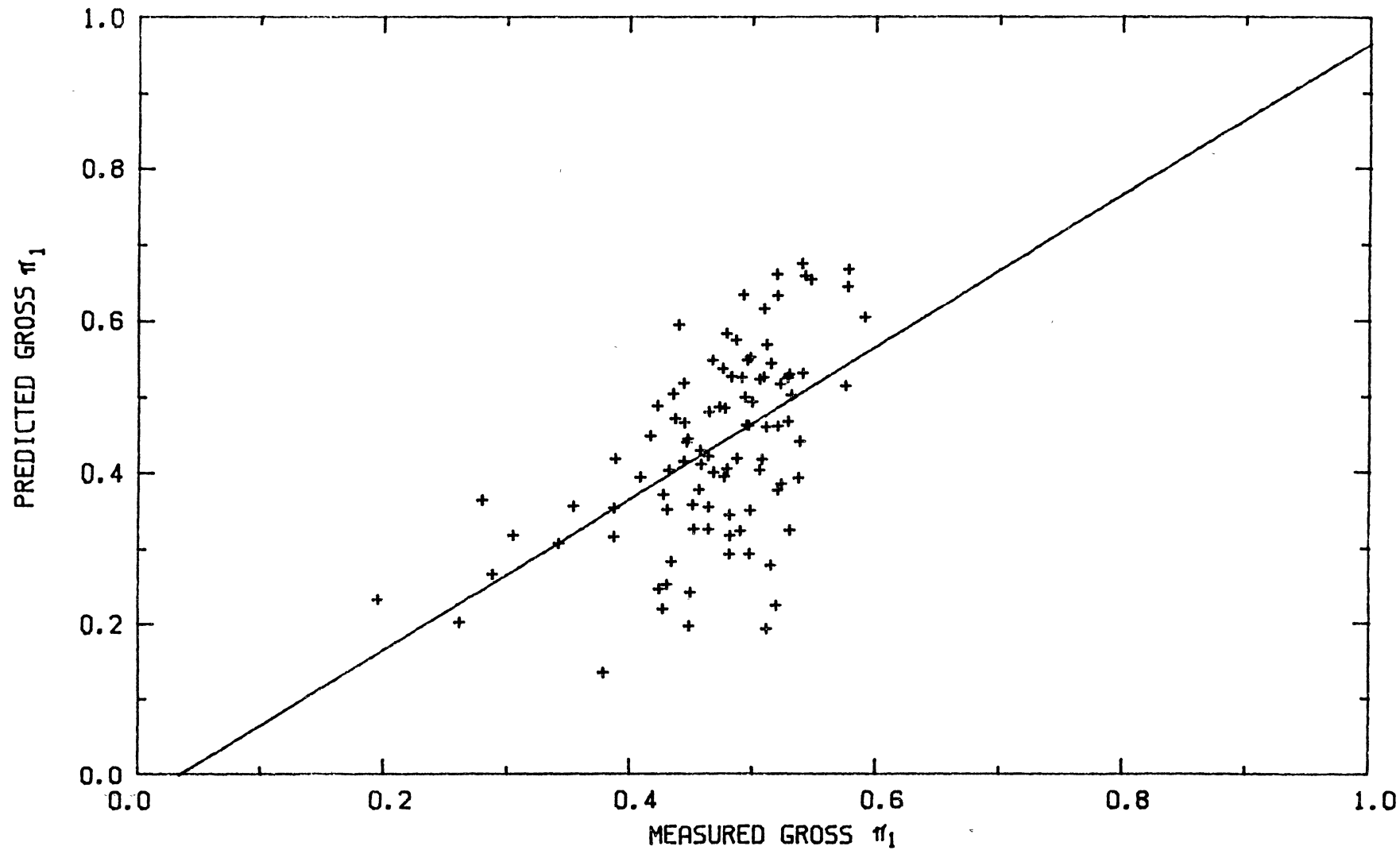


Figure 20. Predicted Gross π_1 versus Measured Gross π_1 for 16.9-30 Tire Only

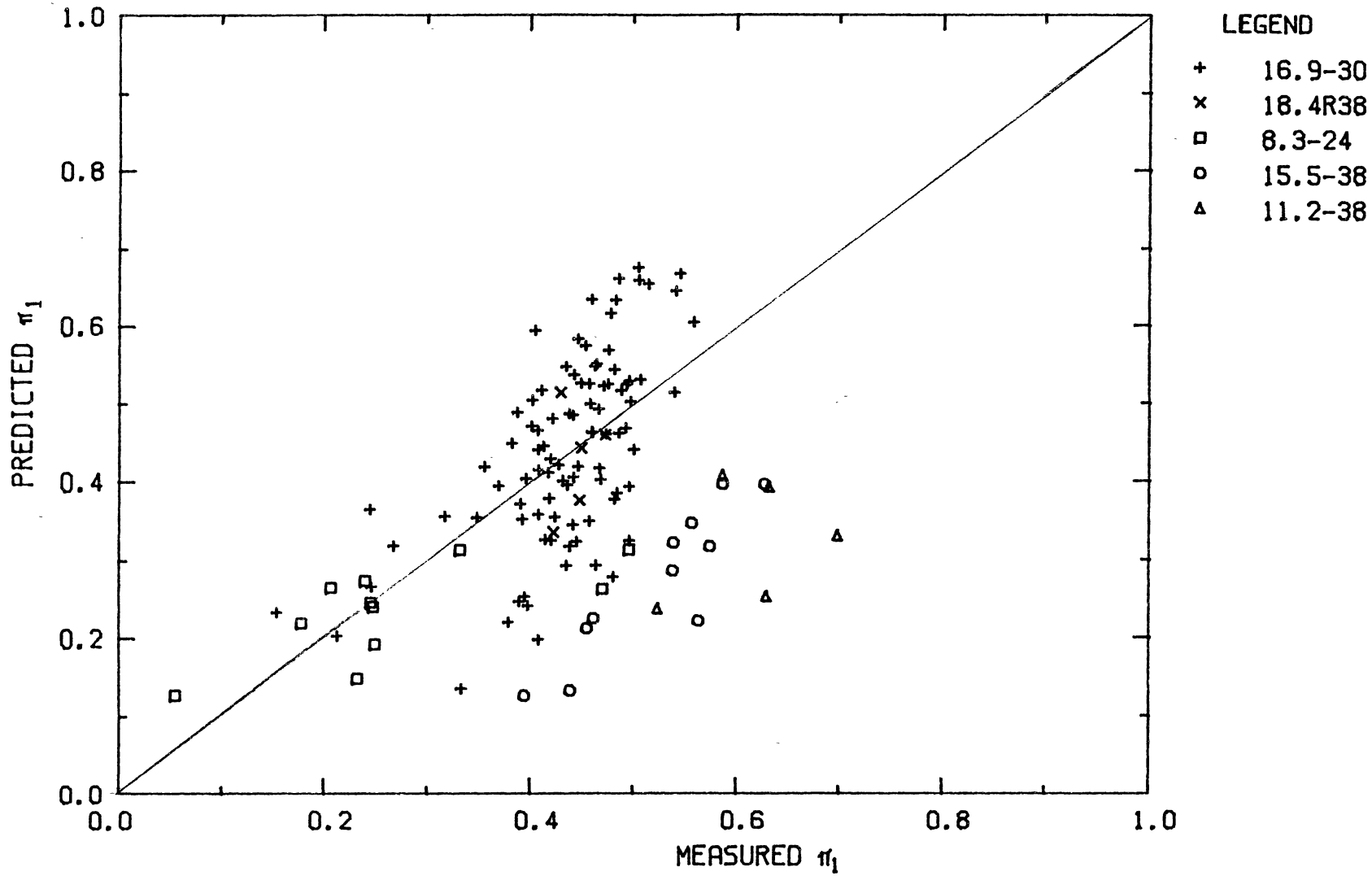


Figure 21. Predicted Gross π_1 versus Measured Gross π_1 for All Five Tires

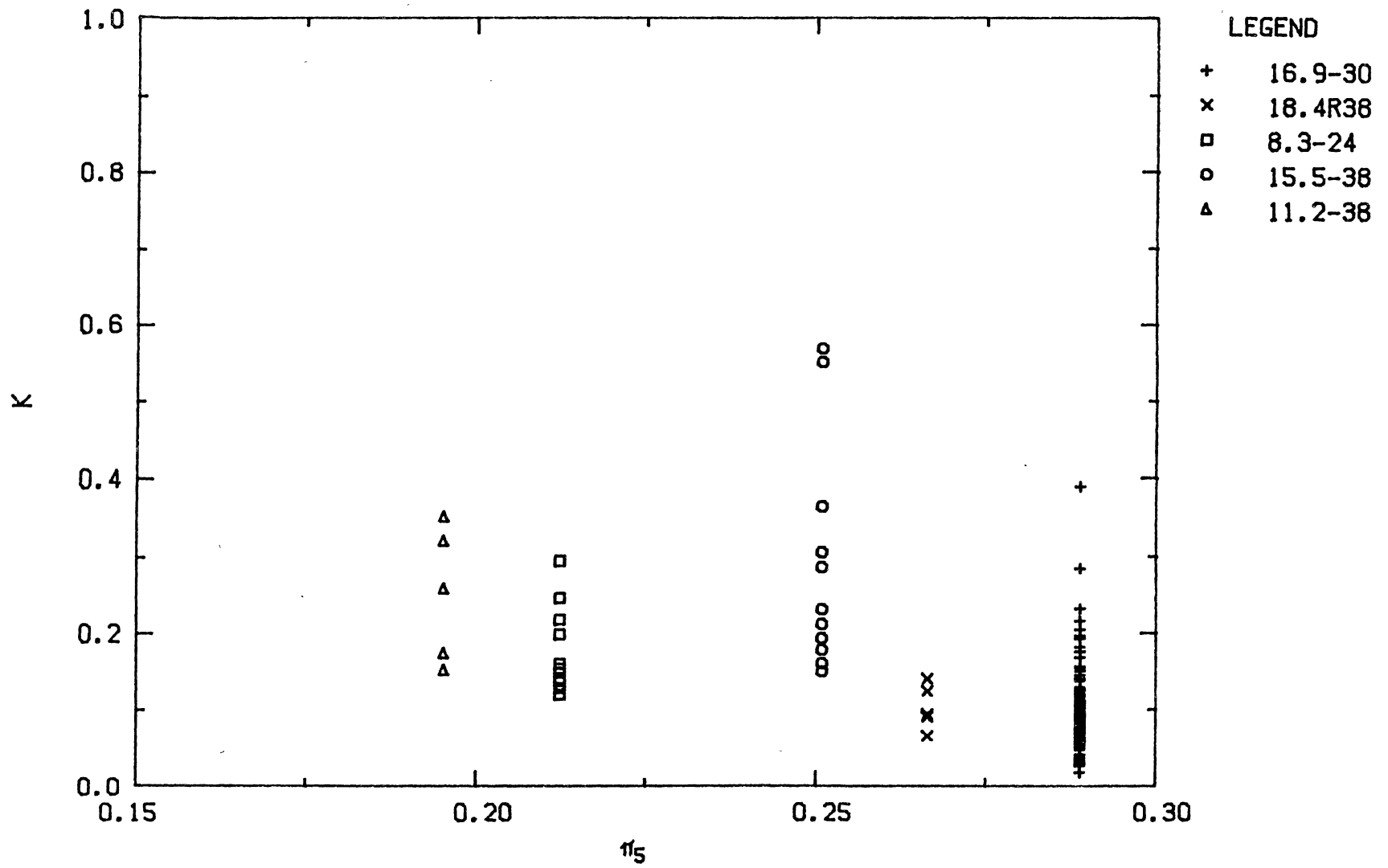


Figure 22. K versus π_5

$$K = -\text{Ln} \left[\frac{\left(1 - \frac{\pi_1}{A}\right)}{\left(\frac{\pi_2 \pi_3}{\pi_4}\right)} \right] \quad (24)$$

and $A=0.677$. No distinct trends are shown in Figure 22 thus illustrating that K is independent of π_5 .

The term A was then plotted against π_5 where:

$$A = \frac{1 - e^{\frac{-K\pi_2\pi_3}{\pi_4}}}{\pi_1} \quad (25)$$

and $K=0.00236$. This plot (Fig. 23) has a good inverse shape except for some strayed points that correspond to the 15.5-38 tire. Gee-Clough, et al. (1976) states that lug height has little affect on tractive performance unless the tire is almost smooth. Since lugs on this tire were worn down to 10 mm in the middle of the tread, it was presumed that this was the contributing factor as to why the data was underpredicted. Linear regression was then performed on A against the inverse of π_5 with the 15.5-38 tire removed from the data set. The resulting equation was:

$$A = -.710 + \frac{0.409}{\pi_5} \quad (26)$$

with an R^2 of 0.210. This equation was then substituted for A in Equation (23). Again predicted data were plotted against measured data to check the quality of fit (Fig. 24). Linear regression yielded the equation:

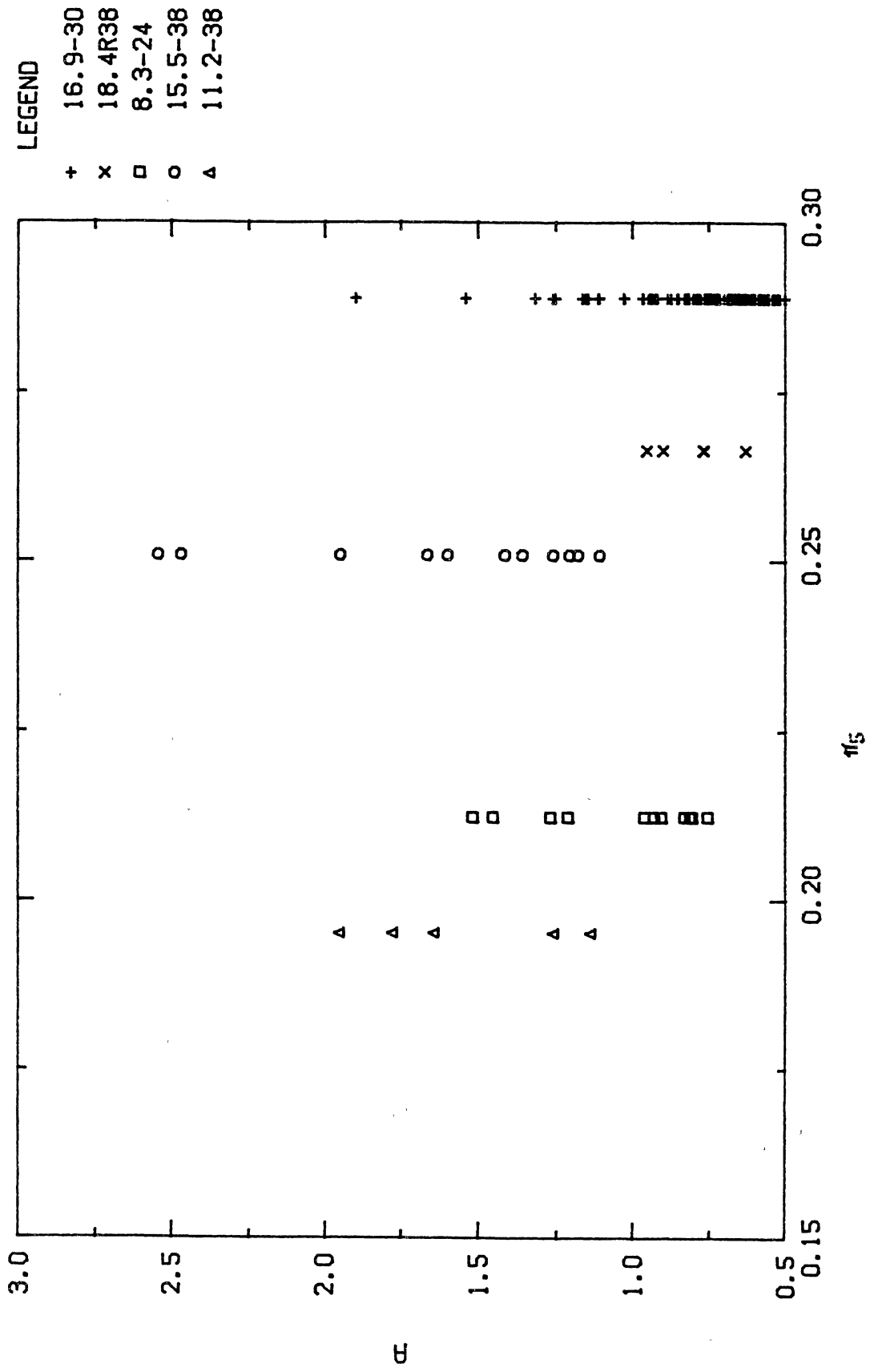


Figure 23. α versus $\pi/5$

$$\pi_1(\text{pred}) = .0504 + .882\pi_1(\text{meas}) \quad (27)$$

with an R^2 of 0.4398. Since the slope of the line is not unity but the intercept approaches zero, this indicates that A is not correct. This can be corrected by dividing Equation (26) by the slope in Equation (27) and substituting this new form of A into Equation (23). The prediction equation then becomes:

$$\pi_1(\text{gross}) = \left(A_1 + \frac{A_2}{\pi_5} \right) \left(1 - e^{-\frac{-K \pi_2 \pi_3}{\pi_4}} \right) \quad (28)$$

$$\begin{aligned} \text{where } A_1 &= -0.805 \\ A_2 &= 0.464 \\ k &= 0.00236 \end{aligned}$$

The final equation has a slope of 1.00 with a zero intercept and an R^2 of 0.450. This plot is shown in Figure 25.

An attempt was made to improve this R^2 by use of NLIN. This was done by solving for the constants in the prediction equation listed above by use of the NLIN procedure. When this was done, the R^2 was increased to 0.456 but the slope of the actual versus predicted gross pull linear regression decreased to 0.43 and the intercept is 0.266. Since the intercept is not equal to zero, the slope cannot be adjusted to one.

When this model was evaluated to see how well it met the boundary conditions, it was found that the velocity term was not behaving as it should at low theoretical

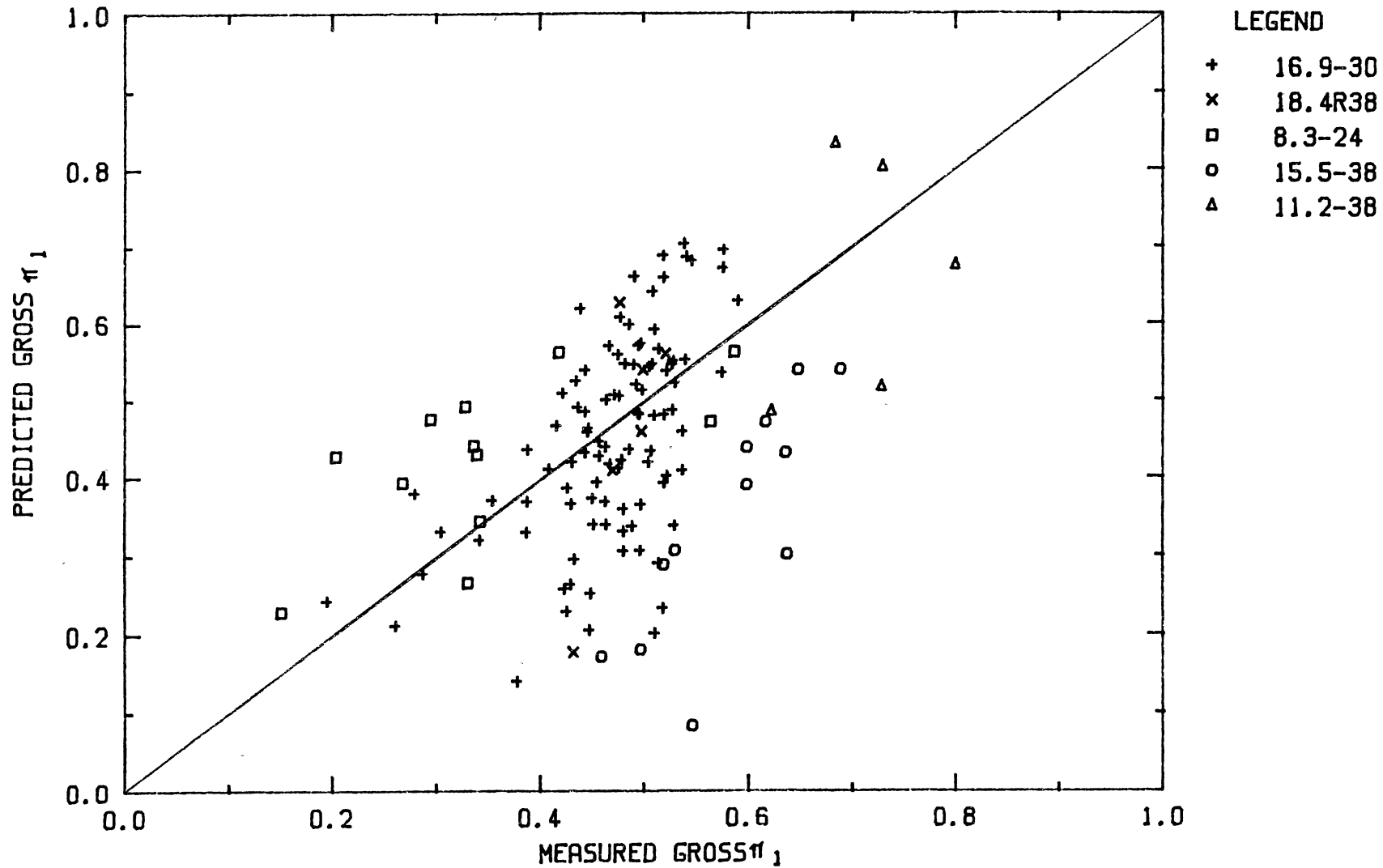


Figure 24. Predicted Gross π_1 versus Measured Gross π_1

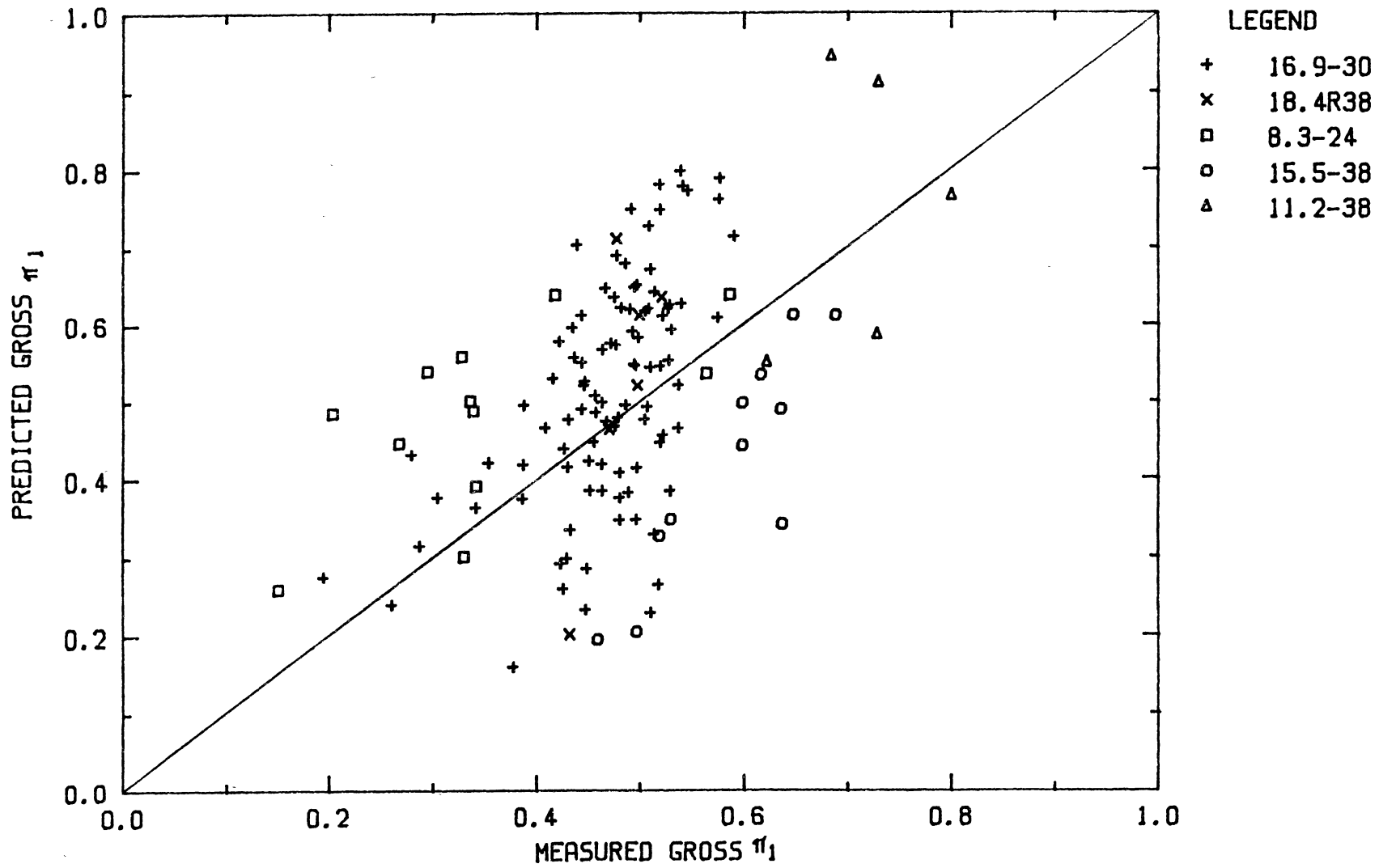


Figure 25. Predicted Gross π_1 versus Measured Gross π_1 with Slope Corrected

velocities. The inverse term used to describe velocity effect was causing the exponential term to approach zero resulting in the net pull to be the asymptotic value times the dynamic load minus the rolling resistance. This would mean that soil strength and wheel slip would have no effect on tractive effort at low velocities. For this reason, this model fails to satisfy the boundary conditions.

Another way to describe tractive effort is to include the rolling resistance into the model by subtracting a zero pull slip value from the actual wheel slip and using the conventional equation form. This is shown in the following form:

$$\pi_1 = A \left[1 - e^{-K\pi_2(\pi_3 - S_0)} \right] \quad (29)$$

When this form is set equal to the form;

$$\pi_1 = A_1 \left(1 - e^{-K\pi_2\pi_3} \right) - \frac{TF}{W} \quad (30)$$

and solved for S_0 with the assumptions:

1. $A = A_1 - \frac{TF}{W}$.
2. K is approximately equal to K_1 .
3. $\frac{TF}{W} = .2292 + \frac{.2337}{\pi_2} - .7038\pi_5$. (12)

then the solution for S_0 is:

$$S_0 = \frac{-\text{Ln} \left(\frac{A}{A + \frac{TF}{W}} \right)}{K\pi_2} \quad (31)$$

This can then be substituted into Equation (29) and used to solve for tractive effort. When this form was entered into

the NLIN procedure, using the data sets with a theoretical velocity of 5.6 to 6.4 km/h on the 16.9-30 tire only, a fit was obtained with:

$$\begin{aligned} A &= .467 \\ K &= .305 \end{aligned}$$

and an R^2 of 0.382. The model developed by NLIN was then used to produce a new K value for each theoretical velocity by the equation:

$$K = \frac{-\text{Ln}\left(1 - \frac{\pi_1}{A}\right)}{\pi_2(\pi_3 - S_0)} \quad (32)$$

and was plotted against π_4 to see if and how theoretical velocity affected the model. This plot is shown in Figure 28. The data formed a curve that had the same form as the curve found in Figure 21. Although an inverse function fit the data, due to the fact that low velocities have no affect on π_1 (Burt and Lyne, 1983), the inverse form would not work. The type of equation found to fit the data best is a modified form of the Witch of Agnesi (Beyer, 1978) which has the form of:

$$K = B_1 + \frac{B_2^3}{\pi_4^2 + B_3^2} \quad (33)$$

The constants were determined by picking 3 points in the data set that the curve would be likely to pass through and solving 3 equations simultaneously. These points are given in Table VII. For π_4 values between 0 and 0.116, a constant K was selected by averaging the data points in

this range. This agrees with trends indicated by Burt and Lyne (1983). The next point was selected by finding the average of the π_4 values and K values that lie within a π_4 range of 0.9 and 1.1. The last point was selected by averaging the high π_4 values shown in Figure 28. The constants found were:

$$\begin{aligned} b_1 &= .1069 \\ b_2 &= .3403 \\ b_3 &= .1857 \end{aligned}$$

A plot of the line formed by this curve is shown with the data in Figure 26.

TABLE VIII
Points Used To Fit Modified
Witch of Agnesi Curve

π_{4b} (Theoretical)	K
$0 < \pi_4 < 0.116$	1.25
1.06	0.142
3.17	0.112

The next step was to determine the effect that π_5 has on the prediction equation. It was shown in Figure 22 that π_5 had no affect on K but seemed to have an affect on A. A

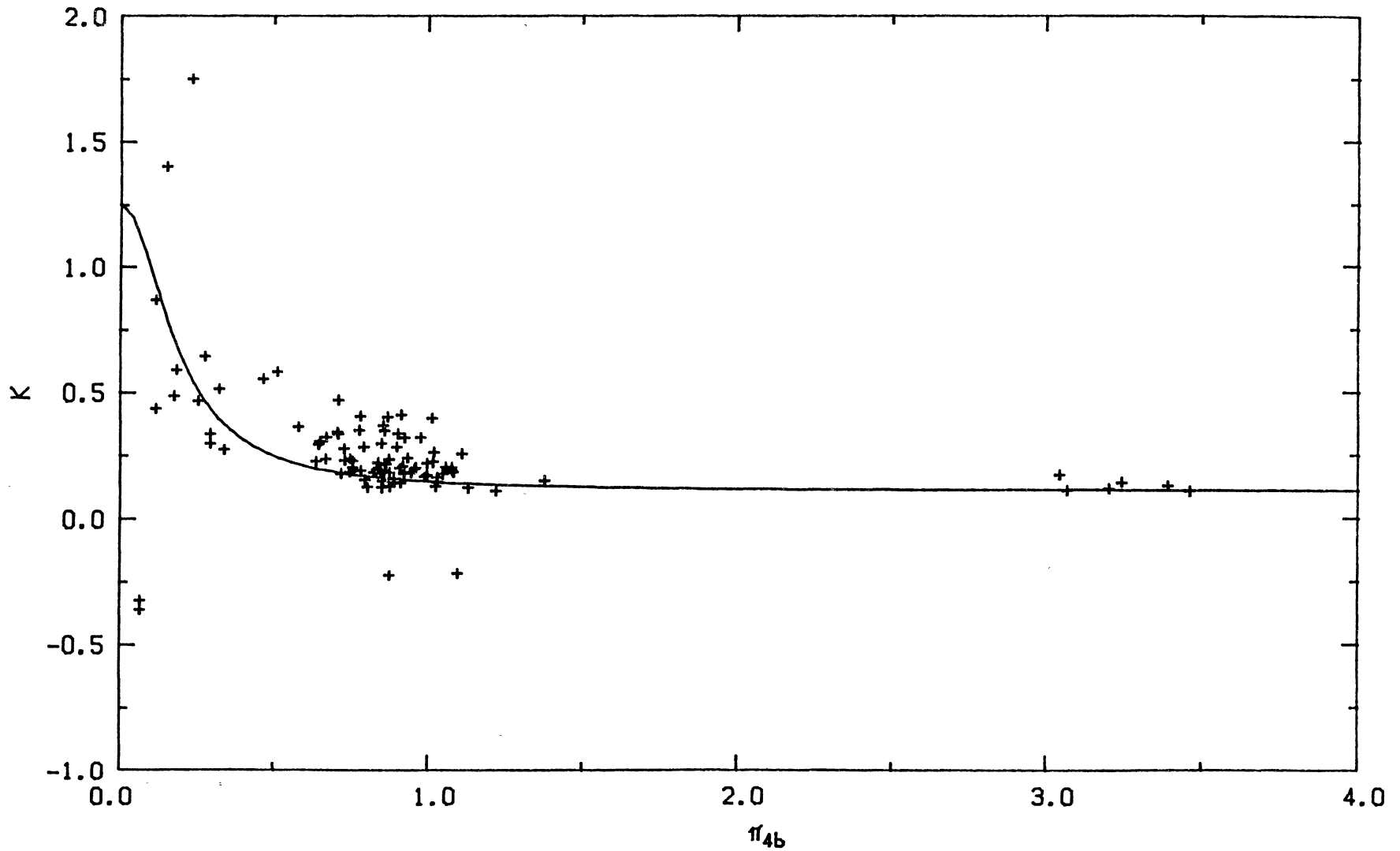


Figure 26. K versus Theoretical π_{4b} With Modified Witch Of Agnesi Curve

was plotted against π_1 where:

$$A = \frac{\pi_1}{\left[1 - e^{-K\pi_2 \pi_3 + \text{Ln}\left(\frac{A}{A + \frac{\text{TF}}{W}}\right)} \right]} \quad (34)$$

Since A appears in both sides of Equation (34), an iterative procedure was used to obtain A. This was done by solving for a new A, setting the old A equal to the new A, then using this new A to solve for another new A. This iterative procedure was repeated until the old A and the new A were within 0.0001 of each other. After plotting (Fig 27), it was found that an inverse relationship fit the data best. Therefore:

$$A = C_1 + \frac{C_2}{\pi_5} \quad (35)$$

$$\begin{aligned} \text{where: } C_1 &= 0.0823 \\ C_2 &= 0.162 \\ R^2 &= 0.151 \end{aligned}$$

was substituted into the general prediction Equation (29).

After substituting in all of the terms into the general prediction equation, the model becomes:

$$\pi_1 = A \left\{ 1 - e^{-K\pi_2 \left[\pi_3 + \text{Ln}\left(\frac{A}{A + \frac{\text{TF}}{W}}\right) \right]} \right\} \quad (36)$$

where A is described by Equation (35), K is described by Equation (33) and TF/W is described by Equation (12).

This form satisfies all boundary conditions used to develop the prediction equation.

To check the validity of Equation (36), predicted π_1

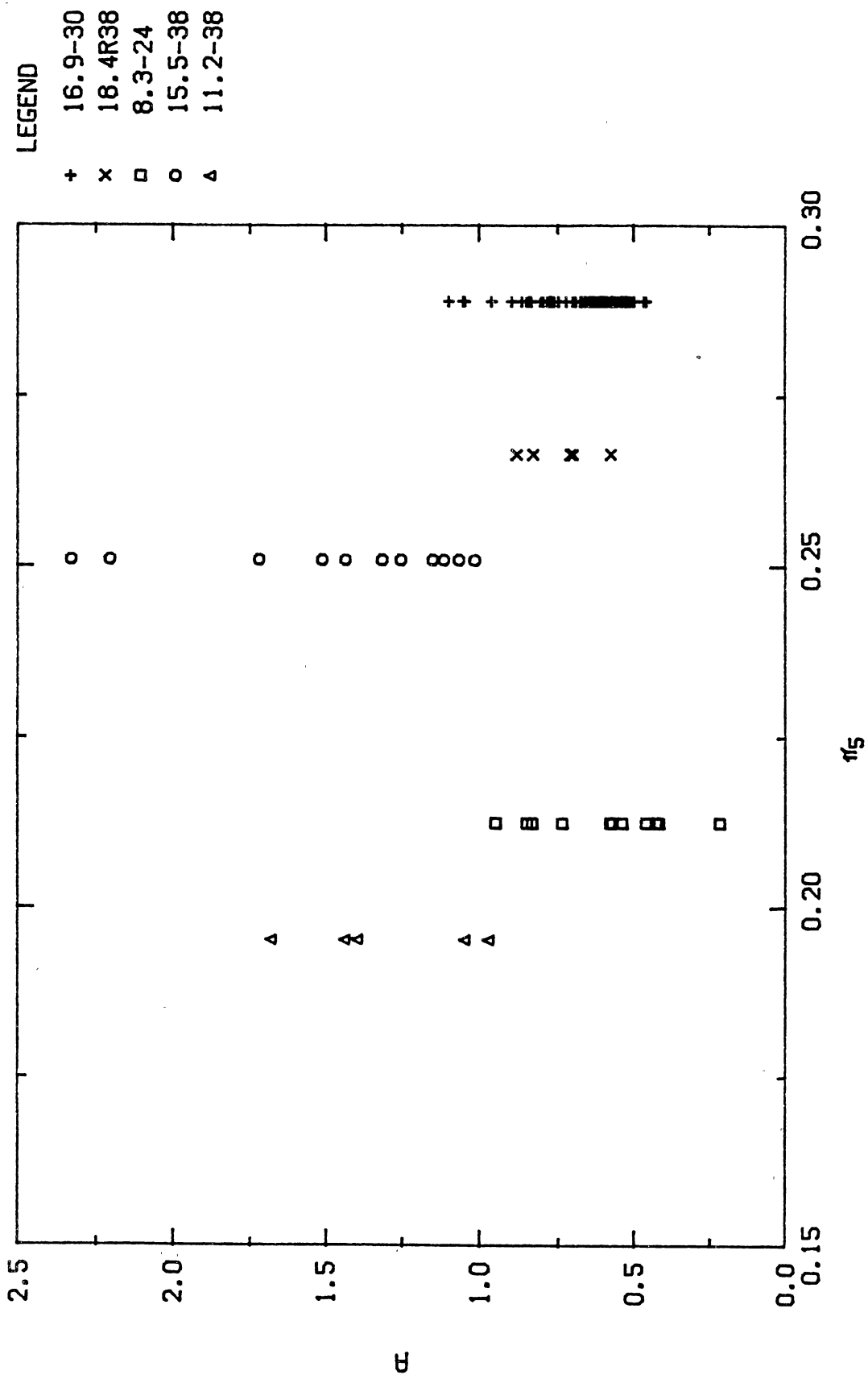


Figure 27. A versus π_s

was plotted against measured π_1 (Fig. 28). Three of the five tires formed a line with a slope of 0.994 and a intercept of -0.04 with a R^2 of 0.49. The other two tires were under predicted believed due to factors not taken into account such as the tire lug height and lug angle.

To check the model for fit of other tires, data for a Firestone 16.5L-16.1, I-3 traction implement tire was used (Appendix J). These data were collected under similar field conditions. The velocities for this tire were less than 1 km/h. A plot was made of predicted π_1 against measured π_1 for this data. This plot (Fig. 29) shows scatter, but the results of the regression are an intercept of 0.06 and a slope of 0.841 with an R^2 of 0.588. This indicates that the prediction equation works for other tires at different velocities.

Figures 30 through 33 shows the effect the four independent π terms have on the dependent π term. Figure 30 shows π_1 plotted against π_2 with the π_3 held at 0.15, π_4 held at 0.142 and π_5 held at 0.289. This plot shows that π_1 increases as π_2 increases to approximately 25, then becomes asymptotic as π_2 continues to increase.

Figure 31 shows π_1 plotted against π_3 with the π_2 held at 25, π_4 held at 0.142 and π_5 held at 0.289. This plot shows that π_1 increases as π_3 increases to approximately

Figure 32 shows π_1 plotted against theoretical velocity, which is the major variable in π_4 , with tire section width held at .43 m, π_2 held at 25, π_3 held at 0.15

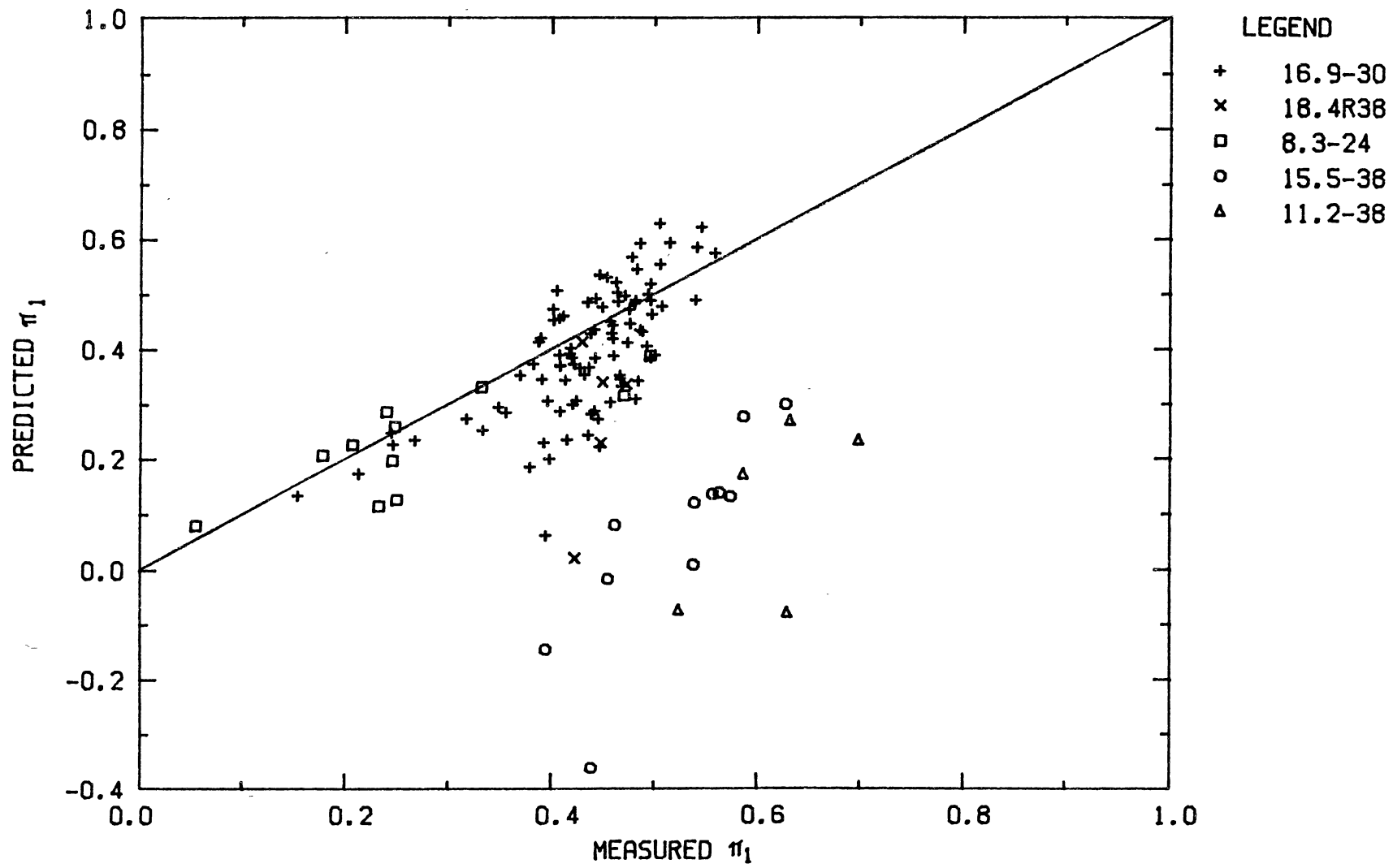


Figure 28. Predicted Net π_1 versus Measured Net π_1

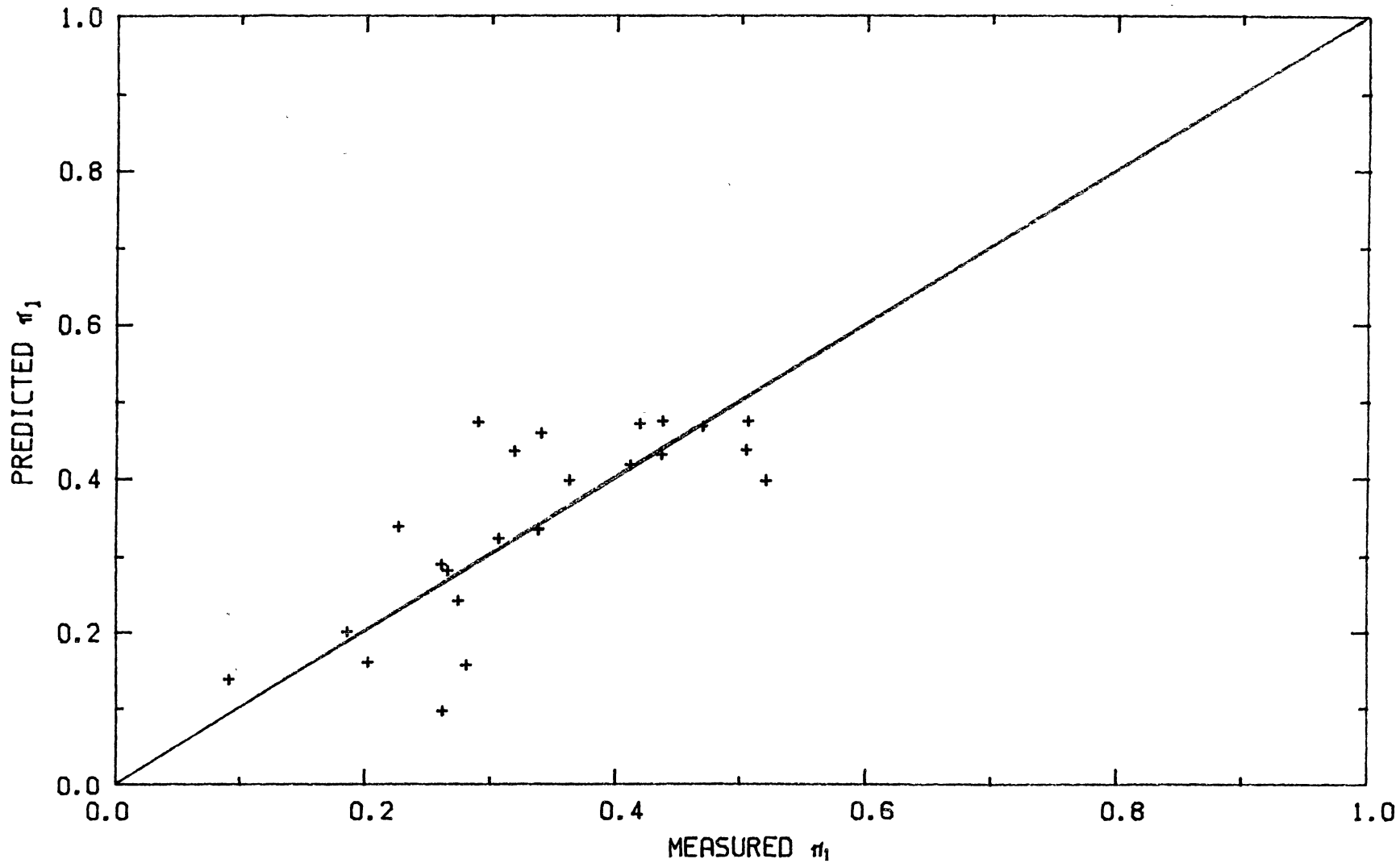


Figure 29. Predicted Net π_1 versus Measured Net π_1 for Firestone 16.5L-16.1, I-3 Traction Implement Tire

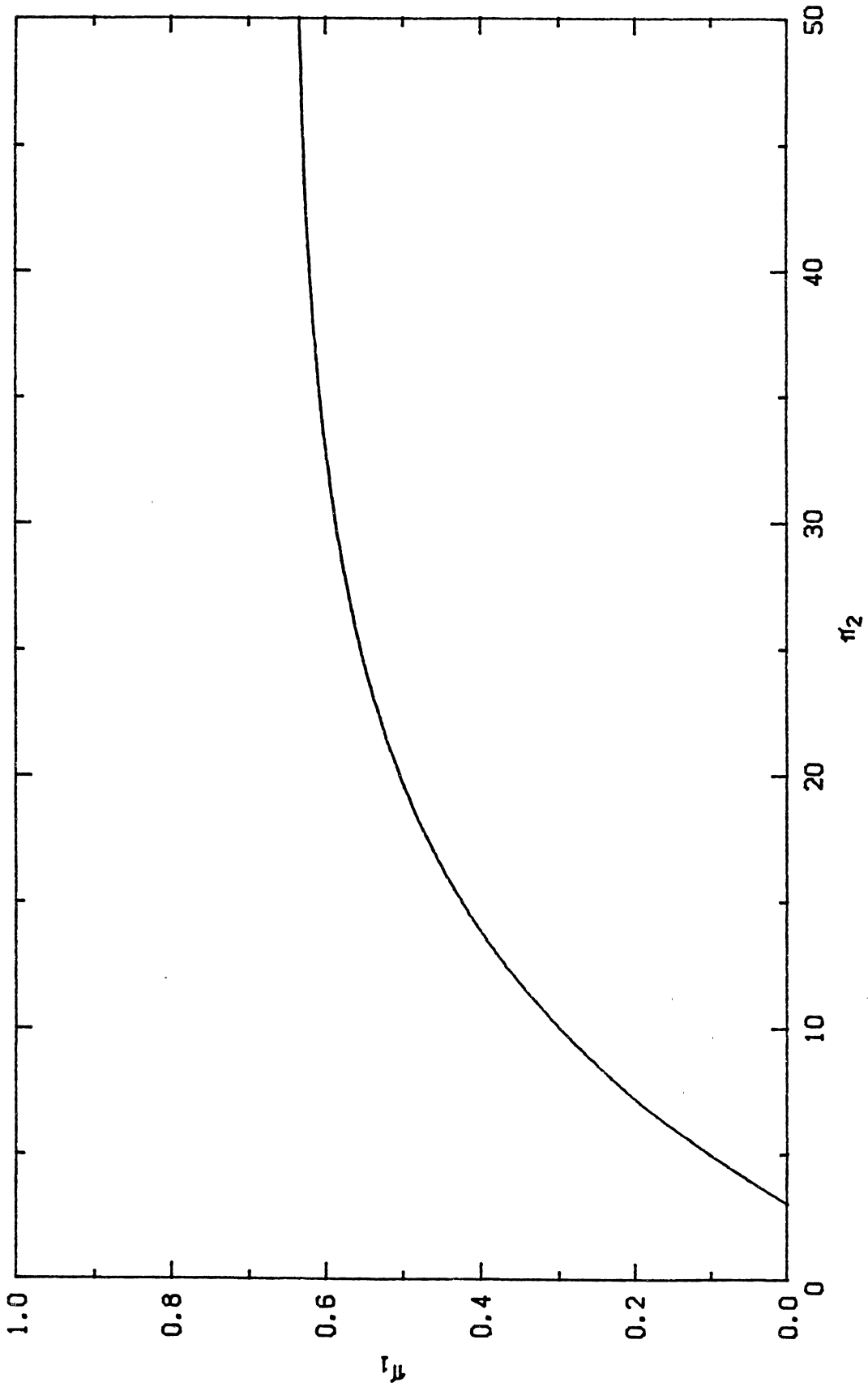


Figure 30. π_1 versus π_2

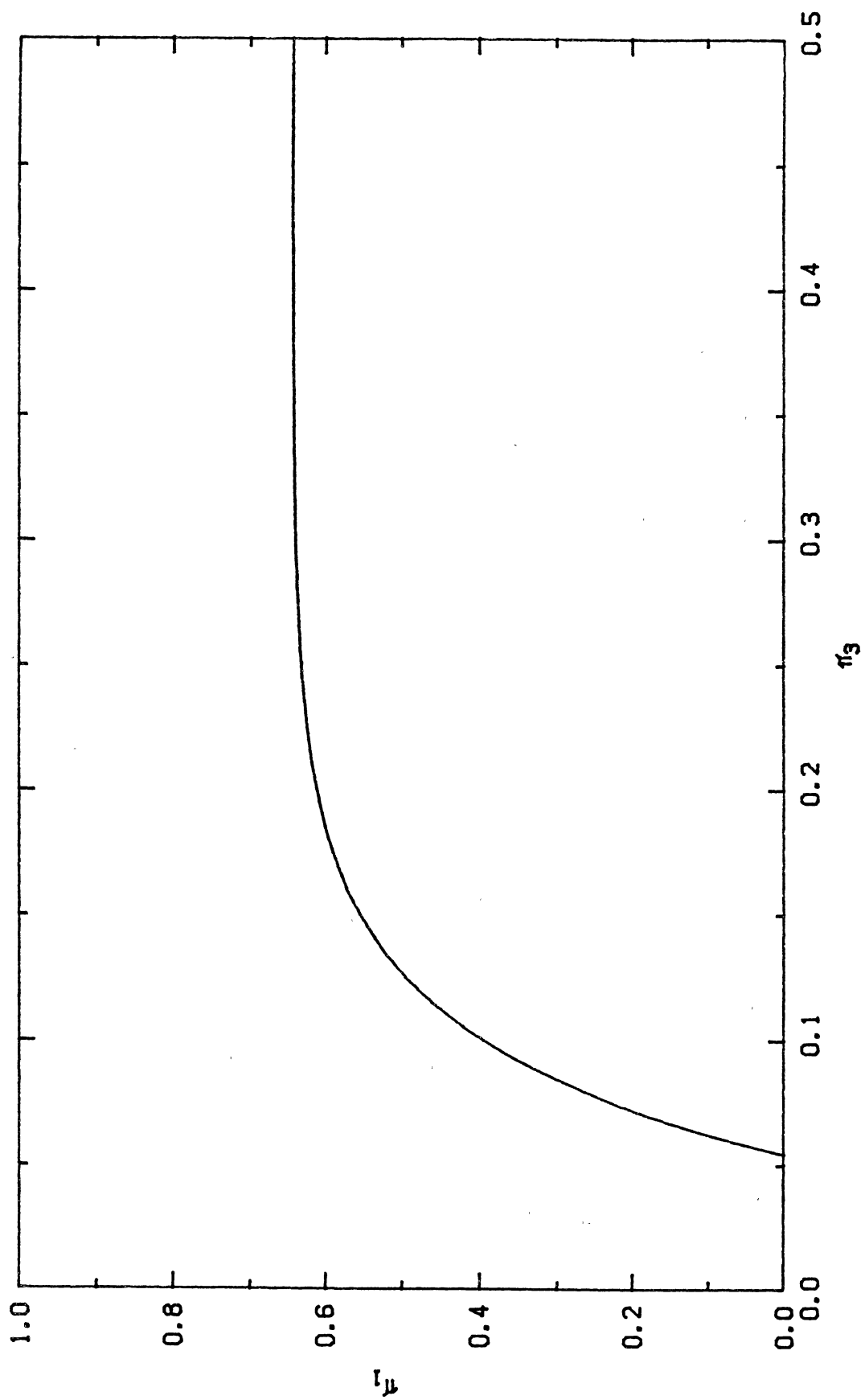


Figure 31. π_1 versus π_3

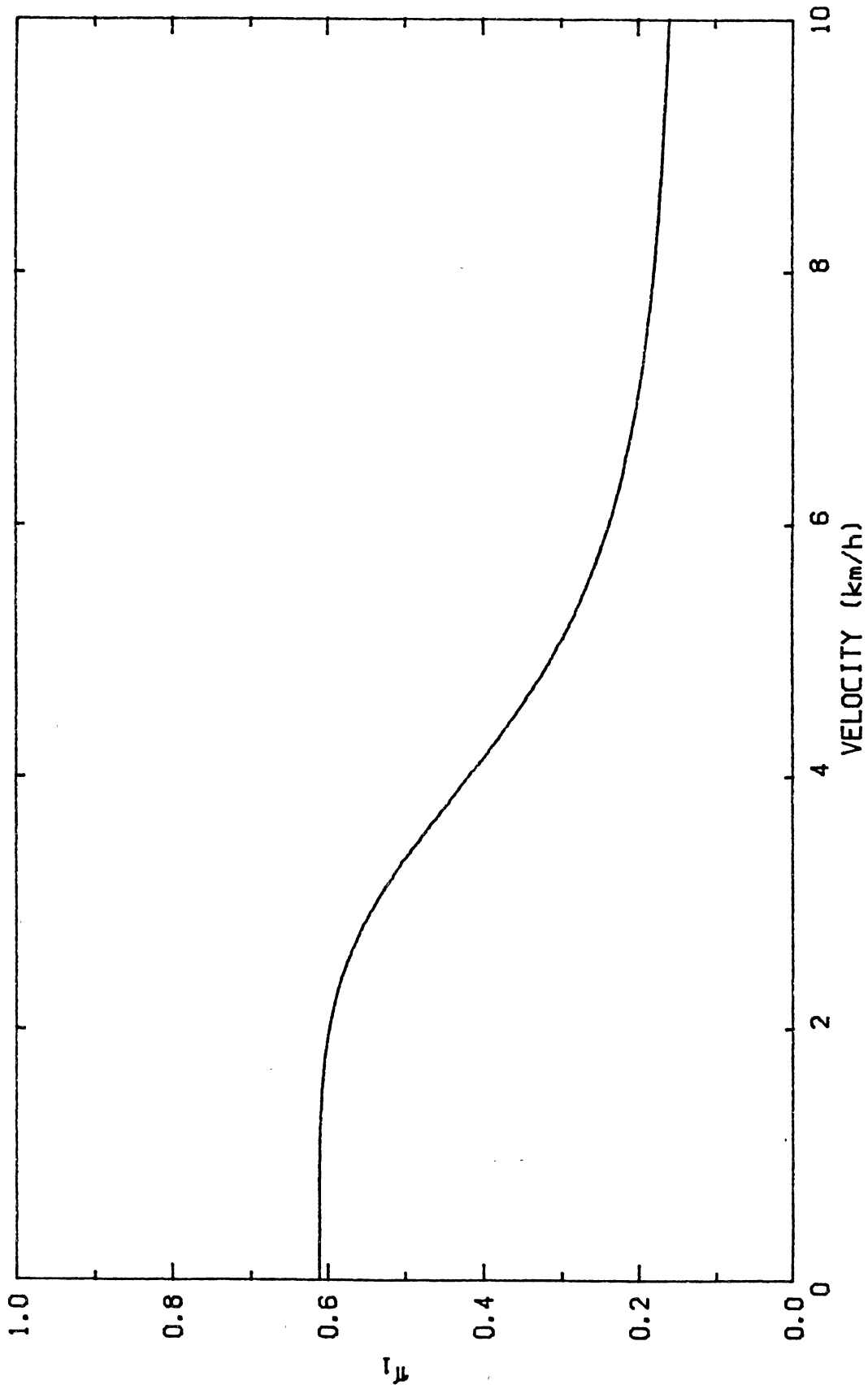


Figure 32. π versus Theoretical Velocity

0.20, then becomes asymptotic as π_3 continues to increase. and π_4 held at 0.142. This plot shows that π_1 remains constant as theoretical velocity increases to about 2 km/h, then decreases as theoretical velocity increases to approximately 7 km/h and becomes asymptotic as theoretical velocity continues to increase.

Figure 33 shows π_1 plotted against π_5 with π_2 held at 25, π_3 held at 0.15 and π_4 held at 0.142. This plot shows that π_1 remains approximately constant as π_5 increases to approximately 0.3 then decreases as π_5 continues to increase.

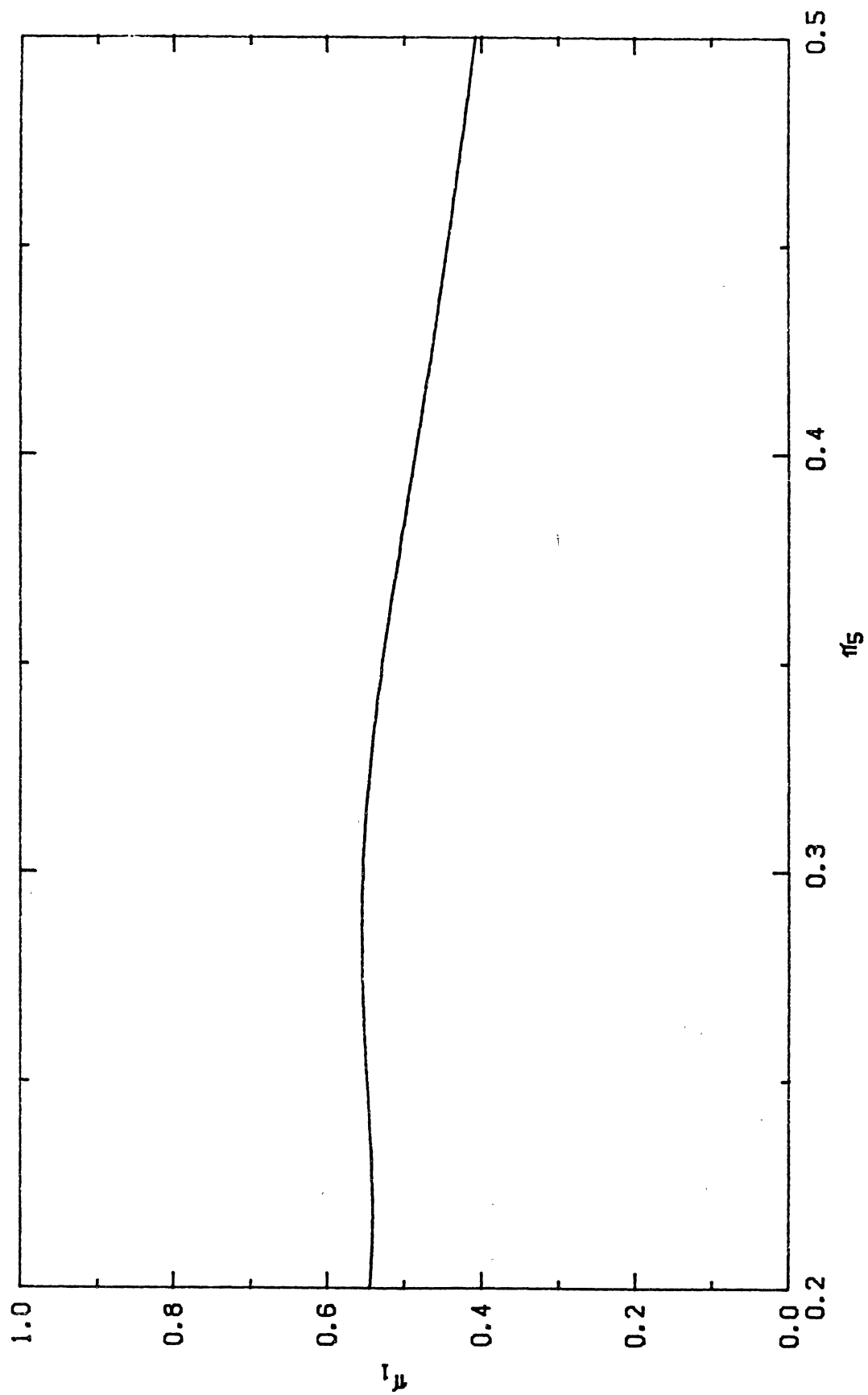


Figure 33. π_1 versus π_5

CHAPTER V

SUMMARY AND CONCLUSIONS

An experimental plan was devised to determine if velocity had an affect on the tractive effort of lugged, agricultural type drive tires. The test was performed at the South Central Research Station, in Chickasha, OK. The machine used was the mobile off-road single tire test apparatus developed at Oklahoma State University. The tire test apparatus measured forward velocity, angular velocity of tested tire, weight transfer and pull developed by the tire. An on-board computer collected the data, stored it on a mini-cassette tape and printed it on paper. Five different tires were tested. Similitude techniques indicated that four π terms were needed to describe the system. When velocity was introduced as a pertinent variable, one more π term was added. An equation was developed to predict tractive force of the agricultural type drive tire.

Prior to testing a tire, a cone penetrometer was used on the test site to get an indication of the soil strength. This was done by measuring cone index values at eight places throughout the length of the plot using an average of the eight measurements over a depth of 15 cm.

A predictable error was found in the data at higher velocities due to a magnetic pickup which measured rotational speed. The data were adjusted for this prior to the analysis. Other sources of error were:

1. Not being able to operate at the prescribed actual and theoretical velocities, thus making it hard to test the desired wheel slips.
2. Not having five tires of equal lug design and wear.
3. Not being able to hold ideal field conditions throughout the field.

The sources of error identified in the data collection process appeared to have minimal affect on the overall research project. The overall prediction equation developed was:

$$\frac{P}{W} = A \left\{ 1 - e^{-KC_n \left[S + \ln \left(\frac{A}{A + \frac{TF}{W}} \right) \right]} \right\}$$

Where:

$$A = 0.823 + \frac{0.162d}{b}$$

$$K = 0.107 + \frac{0.0394}{\left[\left(\frac{v_t}{gb} \right)^2 + 0.0345 \right]}$$

$$\frac{TF}{W} = .2292 + \frac{.2337}{C_n} - .7038 \frac{b}{d}$$

$$C_n = \frac{CIbd}{W}$$

Conclusions derived from this research are:

1. Tractive force decreased as velocity increased in the velocity range of approximately 2 to 7 km/h, but became asymptotic for velocities outside this range.

aspect ratio increased to about 0.3 then decreased as aspect ratio continued to rise.

3. Tractive force increased with wheel slip to approximately 0.20 then became asymptotic as slip continued to rise.

4. Tractive force increased with wheel numeric to approximately 25 then became asymptotic as wheel numeric continued to rise.

5. The final prediction equation was determined to be valid by predicting the pull-to-dynamic load ratio for a tire other than those used in this research.

CHAPTER VI

SUGGESTIONS FOR FURTHER RESEARCH

Further research should be conducted in three areas:

1. Different field conditions.
2. Different selection of tires.
3. Classification of different tires.

The relationship between tractive forces and ground cover, moisture content and soil type should be examined more closely. This will allow a better fitting model. It will also contribute to helping understand the stress-strain behavior of soil.

A different selection of tires with different aspect ratios should also be used at to check the fit of the prediction equation. This will also allow a check to see if the aspect ratio is properly modeled in the prediction equation.

Studies should be conducted to characterize lugged tractor tires. This should involve looking at the lug pattern, distance between lugs, lug height, lug angle, tire section width and tire diameter. Currently, the only factor differentiating lugged tractor tires is the aspect ratio. This assumes that all lug patterns and lug heights react the same. This will greatly help in tire design and

prescribing a design of tire for a specific type of work
and surface condition.

REFERENCES CITED

- Bekker, M.G. 1969. Introduction to terrain-vehicle systems. pp 68. University of Michigan Press, Ann Arbor, MI 49158.
- Beyer, W.H. 1978. CRC standard mathematical tables. pp 325. CRC Press, Inc. West Palm Beach, FL 33409.
- Bloome, P.D., J.D. Summers, A. Khalilian and D.G. Batchelder. 1983. Ballasting recommendations for two-wheel and four-wheel drive tractors. ASAE Paper No. 83-1067. ASAE, St. Joseph, MI 49085.
- Brixius, W.W. and R.D. Wismer. 1978. The role of slip in traction. ASAE Paper No. 78-1538. ASAE, St. Joseph, MI 49085.
- Burt, E.C. and P.W. Lyne. 1983. Velocity effects on traction performance. ASAE Paper No. 83-1556. ASAE, St. Joseph, MI 49085.
- Charles, S.M. and D.J. Schuring. 1984. An empirical model for predicting the effective rolling radius of agricultural drive tires. ASAE Paper No. 84-1555. ASAE, St. Joseph, MI. 49085.
- Clark, R.L. 1985. Tractive modeling with the modified Wismer and Luth equation. ASAE Paper No. 85-1049. ASAE, St. Joseph, MI 49085.
- Draper, N.R. and H. Smith. 1966. Applied regression analysis. John Wiley and Sons, Inc. New York, NY 10016.
- Dwyer, M.J., D.W. Evernder and M. McAllister. 1976. Handbook of agricultural tyre performance. Report No. 18. National Institute of Agricultural Engineering. Silsoe, England.
- Gee-Clough, D., M. McAllister and D.W. Evernden. 1976. The effect of lug height on the tractive performance of tractor drive wheel tyres. Departmental Note Dn/T/679/ 01415. National Institute of Agricultural Engineering. Silsoe, England.

- Gee-Clough, D., M. McAllister and D.W. Evernden. 1977. The effect of forward speed on tractive performance of tractor drive wheel tyres. Departmental Note Dn/t/787/01002. National Institute of Agricultural Engineering. Silsoe, England.
- McAllister, M., D. Gee-Clough and D.W. Evernden. 1976. The effect of aspect ratio on the tractive performance of tractor driving wheel tyres. Departmental Note Dn/t/708/1415. National Institute of Agricultural Engineering. Silsoe, England.
- Murphy, G. 1950. Similitude in engineering. pp 36-38. The Ronald Press Company. New York, NY 10017.
- Reed, I.F., G.E. Vanden and W.F. McCreery. 1964. Effect of tire diameter on performance. National Tillage Machinery Laboratory, Auburn, AL 36849.
- Riethmuller, G.P., D.G. Batchelder, P.D. Bloome. 1982. Microcomputer system for soil strength measurement. ASAE Paper No. 82-3042. ASAE, St. Joseph, MI 49085.
- SAS Institute Inc. 1982. Statistical analysis system user's guide. pp 28-36. Cary, NC 27511.
- Steiner, M. and W. Sohne. 1979. Calculation of the load capacity of tractor tires as well as the medium pressure in the contact area and the rolling resistance on rigid surface. Grundl. Landtechnik 29(5):145-152
- Summers, J.D., D.G. Batchelder, and B.W. Lambert. 1986. Second generation tractor performance monitor. APPLIED ENGINEERING IN AGRICULTURE. 2(1):30-32.
- Wisner, R.D. and H.J. Luth. 1974. Off-road traction prediction equation for wheeled vehicles. TRANSACTIONS of the ASAE 17(1):8-10,14.
- Yong, R.N., E.A. Fattah and N. Skiadas. 1984. Vehicle traction mechanics. Elsevier Science Publishers. New York, NY 10017.

APPENDIX A

BASIC PROGRAM FOR TIRE

TEST MACHINE

Variable Description

A1\$(1) - A6\$(6)	= computer display variable names
B1 - B6	= load transducer regression slopes
A1 - A6	= load transducer regression intercepts
BT & CT	= regression coef. for torque transducer
AA\$	= dummy variable name for display
ZL & XZ	= display line number (0-3)
A\$	= tape file name
T1\$ & TS\$	= tire size
I1\$ & IP	= tire inflation pressure
S2\$ & SL	= static load
R1\$ & RR	= rolling radius
RT\$	= rep. and treatment no.
CL	= cone index level loop no. (1-3)
ZV	= dummy variable
IR & IL	= memory location indexing variable
R(1) - R(7)	= transducer readings
MT	= mean torque
P1 - P3	= pull load on transducers 1-3
V1 - V3	= vertical load on transducers 1-3
MV	= mean vertical load
MR	= dynamic load
MP	= mean pull
NA	= axle speed
VA	= actual vehicle speed
WS	= wheel slip
PW	= pull to weight ratio
TE	= tractive efficiency
AT\$	= repeat or discontinue program variable

Computer Program

```
10 POKE 4,176
20 POKE 5,222
30 A1$(1)=" THIS IS THE TIRE TEST DATA PROGRAM  "
40 A1$(2)=" START OF DATA ACQUISTION           "
```

```

50  A1$(3)="  ENTER TAPE FILE NAME AS ##          "
80  A1$(6)="  ENTER TIRE SIZE AS XX.X-XX OR XX.XRXX "
90  A1$(7)="  ENTER TIRE INFLATION PREASURE        "
100 A1$(8)="  ENTER STATIC LOAD IN POUNDS          "
110 A1$(9)="  ENTER ROLLING RADIUS IN INCHES        "
120 A2$(1)="                                     "
130 A2$(2)="  ENTER REP AND TRT AS XXXX            "
140 A2$(3)="  PRESS 'S' TO START DATA COLLECTION  "
150 A2$(4)="  DO YOU WANT TO MAKE ANOTHER TEST? (Y/N)"
160 A3$(1)="SPEED          "
170 A3$(2)="PULL          "
180 A3$(3)="ROTATION      "
190 A3$(4)="TE            "
200 A4$(1)=" MPH  SLIP    "
210 A4$(2)=" LBS  TORQUE  "
220 A4$(3)=" RPM  P/W     "
230 A4$(4)=" %    PLOT    "
240 A5$(1)=" %          "
250 A5$(2)=" LB-IN"     "
260 A5$(3)="           "
270 A5$(4)="           "
280 CT=65535
330 B1=-4.141149 :A1=16515
333 BT=2.340883772
335 B2=-4.076057 :A2=14434.93
337 B3=-5.88198  :A3=17788.24
340 B4=-.6734546 :A4=2140.45
345 B5=-.7332961 :A5=2697.42
350 B6=1.693858  :A6=-1998.408
380 AA$=A1$(1)
390 ZL=3
400 GOSUB 2410
410 AA$=A2$(1)
420 ZL=1
430 GOSUB 2410
490 AA$=A1$(3)
500 ZL=1
510 GOSUB 2410
520 INPUT A$
530 POKE 42030,ASC(LEFT$(A$,1))
540 POKE 42031,ASC(LEFT$(A$,2,1))
550 POKE 42010,0
560 POKE 42011,64
570 POKE 42012,120
580 POKE 42013,64
800 SN=1
900 AA$=A1$(6)
910 ZL=1
915 GOSUB 2410
920 INPUT T1$
930 IF T1$="" THEN 994
940 TS$=T1$
994 AA$=A1$(7)
995 ZL=1

```

```
996 GOSUB 2410
997 INPUT I1$
998 IF I1$=" " THEN 1010
1000 IP=VAL(I1$)
1010 AA$=A1$(8)
1020 ZL=1
1030 GOSUB 2410
1040 INPUT S2$
1050 IF S2$=" " THEN 1070
1060 SL=VAL(S2$)
1070 AA$=A1$(9)
1080 ZL=1
1090 GOSUB 2410
1100 INPUT R1$
1110 IF R1$=" " THEN 1130
1120 RR=VAL(R1$)
1130 AA$=A2$(2)
1140 ZL=1
1150 GOSUB 2410
1160 INPUT RT$
1250 ZL=1
1251 AA$=A2$(2)
1252 GOSUB 2410
1255 FOR CL=(VAL(MID$(RT$,1,1))) TO 3
1260 AA$=A2$(3)
1261 ZL=0
1262 GOSUB 2410
1263 GET A$: IF A$=<>"S" THEN 1263
1264 AA$=A1$(2)
1265 ZL=0
1266 GOSUB 2410
1267 ZL=1
1268 AA$=A2$(1)
1269 GOSUB 2410
1270 ZL=2
1271 GOSUB 2410
1275 POKE 4,0
1280 POKE 5,124
1290 ZV=USR(WD)
1300 POKE 4,0
1310 POKE 5,222
1311 AA$=A2$(1)
1312 ZL=0
1313 GOSUB 2410
1314 PRINT "DONE"
1320 POKE 4,0
1330 POKE 5,127
1335 ZV=USR(WD)
1350 POKE 4,176
1351 POKE 5,222
1352 I=0
1353 FOR X=29844 TO 29870
1354 POKE 28416 + I + (CL-1)*31,PEEK(X)
1355 I=I+1
```

```
1356 NEXT X
1357 FOR X=27392 TO 27395
1358 POKE 28416 + I + (CL-1)*31,PEEK(X)
1359 I=I+1
1350 NEXT X
1351 NEXT CL
1370 FOR CL=(VAL(MID$(RT$,1,1))) TO 3
1374 CL$=STR$(CL)
1375 RT$=MID$(CL$,2,1)+MID$(RT$,2,3)
1380 IR=(CL-1)*31
1385 FOR X = 1 TO 7
1387 R(X) = PEEK(28416+IR)*65536+PEEK(28423+IR)*256
        +PEEK(28430+IR)
1390 IR=IR+2
1392 NEXT X
1395 MT=(-2039+BT*R(1)/768)/SR(SN)
1397 P1=R(2)*B1/768+A1
1400 P2=R(3)*B2/768+A2
1402 P3=R(4)*B3/768+A3
1405 V1=R(5)*B4/768+A4
1407 V2=R(6)*B5/768+A5
1410 V3=R(7)*B6/768+A6
1415 MV=(V1+V2)/2
1416 MR=SL-MV
1417 MP=P1+P2-P3
1418 IR=(CL-1)*31
1420 NA=(CT-PEEK(28445+IR)*256-PEEK(28446+IR))*SR(SN)
        *.434520242
1425 IF NA<.001 THEN NA=1
1430 VA=(CT-PEEK(28443+IR)*256-PEEK(28444+IR))*0.034842575
1435 IF VA<.01 THEN VA=1
1440 WS=(1-VA*168.06776/(NA*RR))*100
1450 PW=MP/MR
1460 TE=MP*VA*168.06776/(MT*NA)
1470 NA$=STR$(INT(NA*100+.5)/100)
1480 FOR X=LEN(NA$) TO 5
1490 NA$=" "+NA$
1500 NEXT X
1520 VA$=STR$(INT(VA*1000+.5)/1000)
1530 FOR X=LEN(VA$) TO 5
1540 VA$=" "+VA$
1550 NEXT X
1560 WS$=STR$(INT(WS/1000+.5)*1000)
1570 FOR X=LEN(WS$) TO 5
1580 WS$=" "+WS$
1590 NEXT X
1600 PW$=STR$(INT(PW*10000+.5)/10000)
1610 FOR X=LEN(PW$) TO 5
1610 PW$=" "+PW$
1620 NEXT
1630 TE$=STR$(INT(TE*10000+.05)/10000)
1640 FOR X=LEN(TE$) TO 5
1650 TE$=" "+TE$
1660 MT$=STR$(INT(MT+.5))
```

```
1670 FOR LEN(MT$) TO 5
1680 MT$=" "+MT$
1690 NEXT
1730 MP$=STR$(INT(MP+.5))
1740 FOR LEN(MP$) TO 5
1750 MP$=" "+MP$
1760 NEXT
1810 IP$=RIGHT$(STR$(IP),2)
1820 SL$=STR$(INT(SL+.5))
1830 FOR X=LEN(SL$) TO 5
1840 SL$=" "+SL$
1885 GOSUB 2500
1890 RR$=STR$(INT(RR*1000+.5)/1000)
1900 FOR X=LEN(RR$) TO 5
1910 RR$=" "+RR$
1920 NEXT
1921 MV$=STR$(INT(MV+.5))
1922 FOR X=LEN(MV$) TO 5
1923 MV$=" "+MV$
1925 NEXT X
1927 MR$=STR$(INT(MR+.5))
1928 FOR X=LEN(MR$) TO 5
1929 MR$=" "+MR$
1930 NEXT
1933 MM$=STR$(INT(MM+.5))
1934 FOR X=LEN(MM$) TO 5
1935 MM$=" "+MM$
1936 NEXT
1939 FOR IL=1 TO 4
1940 POKE 16383+IL,ASC(MID$(RT$,IL,1))
1950 NEXT
1960 FOR IL= 1 TO 7
1970 POKE 16387+IL,ASC(MID$(TS$,IL,1))
1980 NEXT
1990 FOR IL=1 TO 2
2000 POKE 16394 +IL,ASC(MID$(TS$,IL,1))
2010 NEXT
2020 FOR IL=1 TO 6
2030 POKE 16396+IL,ASC(MID$(SL$,IL,1))
2040 POKE 16402+IL,ASC(MID$(RR$,IL,1))
2050 POKE 16408+IL,ASC(MID$(NA$,IL,1))
2060 POKE 16414+IL,ASC(MID$(VA$,IL,1))
2070 POKE 16420+IL,ASC(MID$(MP$,IL,1))
2080 POKE 16426+IL,ASC(MID$(MT$,IL,1))
2090 POKE 16432+IL,ASC(MID$(WS$,IL,1))
2100 POKE 16438+IL,ASC(MID$(PW$,IL,1))
2110 POKE 16444+IL,ASC(MID$(TE$,IL,1))
2111 POKE 16450+IL,ASC(MID$(MV$,IL,1))
2112 POKE 16456+IL,ASC(MID$(MR$,IL,1))
2113 POKE 16462+IL,ASC(MID$(MM$,IL,1))
2114 POKE 16468+IL,ASC(MID$(P1$,IL,1))
2115 POKE 16474+IL,ASC(MID$(P2$,IL,1))
2116 POKE 16480+IL,ASC(MID$(P3$,IL,1))
2117 POKE 16486+IL,ASC(MID$(V1$,IL,1))
```



```

2118 POKE 16492+IL,ASC(MID$(V2$,IL,1))
2119 POKE 16498+IL,ASC(MID$(V3$,IL,1))
2120 NEXT
2130 A6$(0)=A3$(1)+VA$+A4$(1)+WS$+A5$(1)
2140 A6$(1)=A3$(2)+MP$+A4$(2)+MT$+A5$(2)
2150 A6$(2)=A3$(3)+NA$+A4$(3)+PW$+A5$(3)
2160 A6$(3)=A3$(4)+TE$+A4$(4)+RT$+A5$(4)
2161 A6$(4)="MOMENT "+MM$+" INLB DLOAD "+MR$+" LBS "
2162 A6$(5)="SLOAD "+SL$+" LBS VLOAD "+MV$+" LBS "
2163 A6$(6)="INFPRESS "+IP$+" PSI TIRE "+TS$+" "
2165 IF NA<>1 THEN 2170
2167 PRINT" DRIVE CHAINS OFF"
2170 FOR ZL=0 TO 3
2180 AA$=A6$(ZL)
2190 GOSUB 2410
2200 NEXT
2210 POKE 4,0
2220 POKE 5,221
2230 XZ=USR(YZ)
2240 FOR ZL=0 TO 7
2250 PRINT A6$(ZL)
2260 NEXT
2270 POKE 4,176
2280 POKE 5,222
2290 AA$=A2$(1)
2300 FOR ZL=0 TO 3
2310 GOSUB 2410
2320 NEXT
2324 PRINT"-----"
2325 NEXT CL
2330 AA$=A2$(4)
2340 ZL=1
2350 GOSUB 2410
2360 INPUT AT$
2370 IF AT$="Y" THEN 2391
2380 IF AT$="N" THEN 2400
2390 GOTO 2330
2391 AA$="FOR UNCHANGED INPUTS HIT SPACE-RETURN "
2392 ZL=1
2393 GOSUB 2410
2394 AA$=A2$(1)
2395 ZL=0
2396 GOSUB 2410
2397 FOR I = 1 TO 100
2398 NEXT
2399 GOTO 620
2400 END
2410 FOR ZR=0 TO 39
2420 ZZ$=MID$(AA$,ZR+1,1)
2430 ZX=USR((128+ASC(ZZ$))*256+ZL*64+ZR)
2440 NEXT
2450 RETURN
2455 END
2500 P1$=STR$(INT(P1+.5))

```

```
2505 P2$=STR$(INT(P2+.5))
2510 P3$=STR$(INT(P3+.5))
2515 V1$=STR$(INT(V1+.5))
2520 V2$=STR$(INT(V2+.5))
2525 V3$=STR$(INT(V3+.5))
2530 FOR X=LEN(P1$) TO 5
2535 P1$=" "+P1$
2540 NEXT X
2545 FOR X=LEN(P2$) TO 5
2550 P2$=" "+P2$
2555 NEXT X
2560 FOR X=LEN(P3$) TO 5
2565 P3$=" "+P3$
2570 NEXT X
2575 FOR X=LEN(V1$) TO 5
2580 V1$=" "+V1$
2585 NEXT X
2590 FOR X=LEN(V2$) TO 5
2595 V2$=" "+V2$
2600 NEXT X
2605 FOR X=LEN(V3$) TO 5
2610 V3$=" "+V3$
2620 NEXT X
2630 RETURN
```

APPENDIX B

MACHINE LANGUAGE SUBROUTINE

FOR DATA COLLECTION

Data Storage Locations

Force Data Starts at 4100 (Hex) 16640 (Decimal)
Ends at 6AFF (Hex) 27391 (Decimal)

ie.

\$4100 Transducer #1, Pull (Low Byte)
\$4101 Transducer #1, Pull (High Byte)
\$4102 Transducer #2, Pull (Low Byte)
\$4103 Transducer #2, Pull (High Byte)
\$4104 Transducer #3, Pull (Low Byte)
\$4105 Transducer #3, Pull (High Byte)
\$4106 Transducer #1, Vertical (Low Byte)
\$4107 Transducer #1, Vertical (High Byte)
\$4108 Transducer #2, Vertical (Low Byte)
\$4109 Transducer #2, Vertical (High Byte)
\$410A Transducer #3, Vertical (Low Byte)
\$410B Transducer #3, Vertical (High Byte)
Etc., Repeating this block 767 times

High actual speed count at 6B00 (Hex) 27392 (Decimal)
Low actual speed count at 6B01 (Hex) 27393 (Decimal)
High axle speed count at 6B02 (Hex) 27394 (Decimal)
Low axle speed count at 6B03 (Hex) 27395 (Decimal)

Force Reading Subroutine

Address	Op Code	Operand	Label	Mnemonic	Operand	Remarks
7C00	A9	7F		LDA	##7F	
7C02	8D	3E90		STA	\$903E	DISABLE VIA TIMER INTERRUPTS
7C05	A9	00		LDA	##00	INPUT CONFIGURATION
7C07	8D	3290		STA	\$9032	PORT B
7C0A	A9	20		LDA	##20	SET BIT 5 FOR PULSE COUNTING
7C0C	8D	3B90		STA	\$903B	ACR FOR VIA TIMER 2
7C0F	A9	FF		LDA	##FF	LOW BYTE FOR VIA COUNTER 2
7C11	8D	3890		STA	##9038	ADDRESS FOR LOW BYTE
7C14	A9	FF		LDA	##FF	HIGH BYTE FOR VIA COUNTER 2
7C16	8D	3990		STA	\$9039	HIGH BYTE ADDRESS, STARTS DEC.
7C19	A9	7F		LDA	##7F	DISABLE VIA TIMER INTERRUPTS
7C1B	8D	2E90		STA	\$902E	
7C1E	A9	00		LDA	##00	INPUT CONFIGURATION
7C20	8D	2290		STA	\$9022	PORT B
7C23	A9	20		LDA	##20	SET BIT 5 FOR PULSE COUNTING
7C25	8D	2B90		STA	\$902B	ACR FOR VIA TIMER 2 (COUNTS NEG. PULSES)
7C28	A9	FF		LDA	##FF	LOW BYTE FOR TIMER 2
7C2A	8D	2890		STA	\$9028	ADDRESS FOR LOW BYTE
7C2D	A9	FF		LDA	##FF	HIGH BYTE FOR TIMER 2
7C2F	8D	2990		STA	\$9029	HIGH BYTE ADDRESS, STARTS DEC. RPM COUNT
7C32	A9	00		LDA	##00	BAL FOR DATA ADDRESSING
7C34	85	E0		STA	\$E0	ADDRESS FOR BAL
7C36	A9	41		LDA	##41	BAH FOR DATA ADDRESSING
7C38	85	E1		STA	\$E1	ADDRESS FOR BAH
7C3A	A9	03		LDA	##03	SET INDEX FOR 3 DATA SETS PER PLOT
7C3C	85	E6		STA	\$E6	STORE INDEX AT \$00E6
7C3E	A9	01	D	LDA	##01	"DATA" COUNT (BLOCKS OF 256, DECIMAL)
7C40	85	E2		STA	\$E2	ADDRESS FOR "DATA" INDEX
7C42	A0	00		LDY	##00	ZERO Y REGISTER FOR DATA ADDRESS INDEXING
7C44	A2	00	A	LDX	##00	SET DATA INDEX TO 100
7C46	A9	00	B	LDA	##00	SET MUX TO FIRST CHANNEL

7C48	20	007D	JSR	FR	GO TO FORCE POLLING SUB.
7C4B	A9	01	LDA	##01	SET MUX TO SECOND CHANNEL
7C4D	20	007D	JSR	FR	GO TO FORCE POLLING SUB.
7C50	A9	02	LDA	##02	SET MUX TO THIRD CHANNEL
7C52	20	007D	JSR	FR	GO TO FORCE POLLING SUB.
7C55	A9	03	LDA	##03	SET MUX TO FORTH CHANNEL
7C57	20	007D	JSR	FR	GO TO FORCE POLLING SUB.
7C5A	A9	04	LDA	##04	SET MUX TO FIFTH CHANNEL
7C5C	20	007D	JSR	FR	GO TO FORCE POLLING SUB.
7C5F	A9	05	LDA	##05	SET MUX TO SIXTH CHANNEL
7C61	20	007D	JSR	FR	GO TO FORCE POLLING SUB.
7C64	A9	06	LDA	##06	SET MUX TO SEVENTH
				CHANNEL	
7C66	20	007D	JSR	FR	GO TO FORCE POLLING SUB.
7C69	CA		DEX		
7C6A	D0	DA	BNE	B	GO TO 'B' IF \$100 FORCE
					SETS NOT TAKEN
7C6C	C6	E2	DEC	#E2	
7C6E	D0	D4	BNE	A	GO TO A IF NOT ENOUGH
					DATA BLOCKS TAKEN
7C70	A9	02	LDA	##02	DELAY PARAMETERS
7C72	85	E9	STA	\$E9	
7C74	A9	00	M	LDA	##00
7C76	85	E7	STA	\$E7	
7C78	A9	00	L	LDA	##00
7C7A	85	E8	STA	\$E8	
7C7C	C6	E8	K	DEC	\$E8
7C7E	D0	FC	BNE	K	
7C80	C6	E7	DEC	\$E7	
7C82	D0	F4	BNE	L	
7C84	C6	E9	DEC	\$E9	END OF DELAY
7C86	D0	EC	BNE	M	
7C88	C6	E6	DEC	\$E6	
7C8A	D0	B2	BNE	D	
7C8C	AD	3990	LDA	\$9039	READ SPEED COUNTER HIGH
					ORDER BYTE
7C8F	91	E0	STA	[\$E0],Y	STORE DATA
7C91	20	907D	JSR	AI	DATA ADDRESS INCREASING
					SUB.
7C94	AD	3890	LDA	\$9038	READ SPEED COUNTER LOW
					ORDER BYTE
7C97	91	E0	STA	[\$E0],Y	STORE DATA
7C99	20	907D	JSR	AI	DATA ADDRESS INCREASING
					SUB.
7C9C	AD	2990	LDA	\$9029	READ AXLE SPEED COUNTER
					HIGH ORDER BYTE
7C9F	91	E0	STA	[\$E0],Y	STORE DATA
7CA1	20	907D	JSR	AI	DATA ADDRESS INCREASING
					SUB.
7CA4	AD	2890	LDA	\$9028	READ AXLE SPEEDE COUNTER
					LOW ORDER BYTE
7CA7	91	E0	STA	[\$E0],Y	STORE DATA
7CA9	60		RTS		

7D00	8D	FA9F	FR	STA	\$9FFA	SET MUX CHANNEL
7D03	A9	00		LDA	##00	
7D05	8D	0BA0		STA	\$A00B	ACR SET TIME PULSE ON TIMER 2
7D08	A9	26		LDA	##26	LOW ORDER BYTE OF TIME (CLOCK CYCLES)
7D0A	8D	08A0		STA	\$A008	LOW ORDER BYTE ADDRESS
7D0D	A9	00		LDA	##00	HIGH ORDER BYTE OF TIME
7D0F	8D	09A0		STA	\$A009	HIGH ORDER BYTE ADDRESS, START TIMER 2
7D12	A9	20		LDA	##20	SET BIT 5 OF ACCUMULATOR
7D14	2C	0DA0	E	BIT	\$A00D	TEST TIME OUT SIGNAL
7D17	F0	FB		BEQ	E	TEST AGAIN IF NOT SET YET
7D19	AD	08A0		LDA	\$A008	CLEAR TIMER 2 TIME OUT SIGNAL
7D1C	8D	FB9F		STA	\$9FFB	START A/D CONVERSION
7D1F	A9	02		LDA	##02	START OF 26E-6 SECOND DELAY
7D21	85	E4		STA	\$E4	
7D23	C6	E4	F	DEC	\$E4	
7D25	D0	FC		BNE	F	END OF DELAY LOOP
7D27	EA			NOP		
7D28	EA			NOP		
7D29	EA			NOP		END OF DELAY
7D2A	AD	FE9F		LDA	\$9FFE	READ DATA
7D2D	91	E0		STA	[\$E0],Y	STORE DATA
7D2F	20	907D		JSR	AI	DATA ADDRESS INCREASING
7D32	AD	FD9F		LDA	\$9FFD	
7D35	91	E0		STA	[\$E0],Y	
7D37	20	907D		JSR	AI	
7D3A	60			RTS		
7D90	18		AI	CLC		CLEAR CARRY
7D91	A5	E0		LDA	\$E0	ADL OF DATA ADDRESS
7D93	69	01		ADC	##01	INCREMENT DATA ADDRESS
7D95	85	E0		STA	\$E0	STORE DATA ADL
7D97	A5	E1		LDA	\$E1	ADH OF DATA ADDRESS
7D99	69	00		ADC	##00	INCREMENT ADL IF NECESSARY
7D9B	85	E1		STA	\$E1	STORE DATA ADH
7D9D	60			RTS		

Summed Data Locations

\$7494 - #1,High	\$749D - #2,Medium	\$74A6 - #3,Low
\$7495 - 00	\$749E - #6,High	\$74A7 - #7,Medium
\$7496 - #2,High	\$749F - #3,Medium	\$74A8 - #4,Low
\$7497 - 00	\$74A0 - #7,High	\$74A9 - 00
\$7498 - #3,High	\$74A1 - #4,Medium	\$74AA - #5,Low
\$7499 - 00	\$74A2 - #1,Low	\$74AB - 00
\$749A - #4,High	\$74A3 - #5,Medium	\$74AC - #6,Low
\$749B - #1,Medium	\$74A4 - #2,Low	\$74AD - 00
\$749C - #5,High	\$74A5 - #6,Medium	\$74AE - #7,Low

Speed counts remain in same memory
locations (\$6B00 to \$6B03)

Summation Routine

Address	Op Code	Operand	Label	Mnemonic	Operand	Remarks
7F00	98			TYA		
7F01	48			PHA		
7F02	8A			TXA		
7F03	48			PHA		
7F04	A9	00		LDA	#\$00	STORE VALUE 00 IN
7F06	85	EA		STA	\$EA	LOCATION \$EA
7F08	A9	41		LDA	#\$41	STORE VALUE 41 IN
7F0A	85	EB		STA	\$EB	LOCATION \$EB
7F0C	18			CLC		CLEAR CARRY
7F0D	D8			CLD		CLEAR DECIMAL
7F0E	A0	06		LDY	#\$06	
7F10	A9	00		LDA	#\$00	
7F12	99	9374		STA	\$7493,Y	
7F15	99	9A74		STA	\$749A,Y	ZERO MEMORY LOCATIONS
7F18	99	A174		STA	\$74A1,Y	\$7493 TO \$74AE
7F1B	99	A874		STA	\$74A8,Y	
7F1E	88			DEY		
7F1F	10	F4		BPL	F4	
7F21	A9	03		LDA	#\$03	SET INDEX FOR 3 DATA SETS
7F23	A9	AF74		STA	\$74AF	PER PLOT
7F26	A2	00		LDX	#\$00	ZERO X REGISTAR
7F28	A0	00		LDY	#\$00	ZERO Y REGISTAR
7F2A	18			CLC		CLEAR CARRY
7F2B	B1	EA		LDA	[EA],Y	LOAD ACCUM. WITH [EA]+Y
7F2D	79	A274		ADC	\$74A2,Y	ADD \$74A2+Y TO ACCUM. WITH CARRY

7F30	99	A274	STA	\$74A2,Y	STORE ACCUM. AT \$74A2+Y
7F33	C8		INY		INCREMENT Y
7F34	B1	EA	LDA	[EA],Y	LOAD ACCUM. WITH [EA]+Y
7F36	88		DEY		DECREMENT Y
7F37	79	9B74	ADC	\$749B,Y	ADD \$749B+Y TO ACCUM. WITH CARRY
7F3A	99	9B74	STA	\$749B,Y	STORE ACCUM. AT \$749B+Y
7F3D	A9	00	LDA	#\$00	ZERO ACCUM.
7F3F	79	9474	ADC	\$7494,Y	ADD \$7494+Y TO ACCUM.
7F42	99	9474	STA	\$7494,Y	STORE ACCUM. AT \$7494+Y
7F45	C8		INY		INCREMENT Y
7F46	C8		INY		INCREMENT Y
7F47	C0	0E	CPY	#\$0E	COMPARE Y TO 14
7F49	30	DF	BMI	DF	BRANCH TO \$7F2A IF Y<14
7F4B	18		CLC		CLEAR CARRY
7F4C	A0	00	LDY	#\$0E	LOAD Y REGISTAR WITH 14
7F4E	A5	EA	LDA	\$EA	LOAD ACCUM. WITH \$EA
7F50	69	0E	ADC	#\$0E	ADD TO 14 TO ACCUM. WITH CARRY
7F52	85	EA	STA	\$EA	STORE ACCUM. AT \$EA
7F54	A9	00	LDA	#\$00	ZERO ACCUMULATOR
7F56	65	EB	ADC	\$EB	ADD \$EB TO ACCUM.
7F58	85	EB	STA	\$EB	STORE ACCUM. AT \$EB
7F5A	CA		DEX		DECREMENT X
7F5B	D0	CD	BNE	CD	BRANCH TO \$7F2A IF X≠0
7F5D	CE	AF74	DEC	\$74AF	DECREMENT VALUE IN \$74AF
7F60	D0	C8	BNE	C8	BRANCH TO \$7F2A IF VALUE IN \$74AF ≠ 0
7F62	68		PLA		PULL ACCUM. FROM STACK
7F63	AA		TAX		TRANSFER ACCUM. TO X REGISTAR
7F64	68		PLA		PULL ACCUM. FROM STACK
7F65	A8		TAY		TRANSFER ACCUM. TO Y REGISTAR
7F66	60		RTS		RETURN FROM SUBROUTINE

APPENDIX C

COMPUTER MEMORY MAP FOR TIRE TEST MACHINE

\$0000 - \$3FFF	Reserved for basic program.
\$4000 - \$4078	Memory to be printed to cassette tape.
\$4100 - \$6AFF	Transducer values from data collection subroutine.
\$6B00 - \$6B03	Velocity counts from data collection subroutine.
\$6F00 - \$6F1E	First cone index level data.
\$6F1F - \$6F3D	Second cone index level data.
\$6F3E - \$6F5C	Third cone index level data.
\$7493 - \$74AE	Summed data from sub. \$7F00 - 7F66.
\$7C00 - \$7D9E	Data collection subroutine.
\$7F00 - \$7F66	Summing subroutine.

APPENDIX D

ROLLING RADIUS DATA

Tire Size Infl. Pres.	Load	Number of Revolutions	Distance Traveled	Rolling Radius
(kPa)	(kN)	--	(m)	(m)
16.9-30 (124)	8.36	15	65.78	0.698
	10.81	15	65.24	0.692
	15.52	15	64.01	0.679
	17.97	15	63.56	0.674
	19.09	15	63.37	0.672
18.4R38 (138)	11.45	15	79.75	0.846
	13.90	15	79.60	0.846
	18.61	15	79.07	0.839
	21.06	15	78.94	0.838
	25.78	15	78.64	0.834
8.3-24 (152)	4.693	20	59.16	0.471
	5.427	20	58.55	0.466
	6.338	20	58.09	0.462
15.5-38 (138)	9.10	15	70.67	0.750
	11.54	15	70.28	0.746
	16.26	15	69.32	0.736
	18.70	15	68.91	0.731
	19.82	15	68.75	0.729
11.2-38 (124)	5.32	20	87.08	0.693
	6.44	20	86.71	0.690
	8.30	20	85.75	0.682
	9.42	20	85.30	0.679
	10.74	20	84.79	0.675

APPENDIX E

PROGRAM TO INPUT TIRE TEST

DATA TO IBM-PC

```

10 CLS
20 PRINT
30 PRINT
40 PRINT "                TIRE TEST DATA"
50 PRINT
60 PRINT "                A-----ADD TO FILE"
70 PRINT "                P-----PRINT FILE"
75 PRINT "                E-----END PROGRAM"
76 PRINT "                S-----SPECIAL
80 PRINT "                ?"
90 A$=INKEY$:IF A$="" THEN 90
100 IF A$="A" THEN 135
110 IF A$="P" THEN 340
120 IF A$="E" THEN END
125 IF A$="S" THEN 600
130 GOTO 80
135 OPEN "B:TT.DAT" FOR APPEND AS #1
140 INPUT "PLOT NUMBER";P$
150 IF P$="" THEN CLOSE #1:GOTO 10
160 INPUT "WEIGHT (RETURN IF UNCHANGED)";W$
170 IF W$="" THEN 181
180 WE=VAL(W$)
181 FOR A=1 TO 3
182 P$=MID$(STR$(A),2)+MID$(P$,2,3)
183 PRINT
184 PRINT"  PLOT---"P$
190 INPUT "SPEED";SP
195 IF MID$(P$,2,1)="5" THEN 210
200 INPUT "SLIP";SL
210 INPUT "PULL";P
215 IF MID$(P$,2,1)="5" THEN 230
220 INPUT "TORQUE";T
230 INPUT "VLOAD";VL
250 P=P+123           :REM  PULL CORRECTION FACTOR
260 VL=VL+926        :REM  VERT. LOAD CORRECTION FACTOR
270 T=T-38592!       :REM  TORQUE CORRECTION FACTOR
275 IF MID$(P$,2,1)="5" THEN T=0
280 PW=P/(WE-VL)
285 BEEP:INPUT "THESE VALUES CORRECT";A$
286 IF A$="N" THEN 184

```

```

290 PRINT #1, USING " \ \ #### #.### ##.### #### #####
      #####"; P$, WE, SP, SL, P, T, VL, PW
300 PRINT USING " \ \ #### #.### ##.### #### #####
      .#####"; P$, WE, SP, SL, P, T, VL, PW
320 NEXT
330 GOTO 140
335 CLOSE 1
340 LPRINT " PLOT WGHT SPD SLP PULL
      TRQU VLOAD P/W"
350 LPRINT"-----
      -----"
360 OPEN "B:TT.DAT" FOR INPUT AS 1
370 IF EOF(1) THEN GOTO 500
380 INPUT #1, P$, WE, SP, SL, P, T, VL, PW
390 LPRINT USING " \ \ #### #.### ##.### ####
      ##### .#####"; P$, WE, SP, SL, P, T, VL, PW
400 LPRINT
410 GOTO 370
500 LPRINT CHR$(12)
510 CLOSE #1
520 GOTO 10
600 REM THIS ROUTINE SAVES SLIP vs.P/W FOR PLOTRAX
601 REM FILE NAME IS ON LINE 610
602 REM PLOT NUMBER ON LINE 630
609 OPEN "TT1.DAT" FOR INPUT AS 1
610 OPEN "B:CI3" FOR APPEND AS 2
620 INPUT #1, P$, WE, SP, SL2, P, T, VL, PW2
621 IF EOF (1) THEN 630
622 INPUT #1, P$, WE, SP, SL3, P, T, VL, PW3
623 IF EOF (1) THEN 630
624 INPUT #1, P1$, WE, SP, SL1, P, T, VL, PW1
630 WRITE#2, SL3, PW3
635 PRINT SL3, PW3
640 IF EOF (1) THEN 660
650 GOTO 620
660 CLOSE #1
670 CLOSE #2
680 GOTO 10

```

APPENDIX F

PROGRAM TO INPUT CONE INDEX

DATA TO IBM-PC

```

10  CLS
20  PRINT
30  PRINT
40  PRINT "      CONE INDEX INPUT AND REVIEW PROGRAM"
50  PRINT
60  PRINT
70  PRINT "      TASK TO BE PERFORMED:"
80  PRINT
90  PRINT "          A----ADD DATA TO EXISTING DATA FILE"
100 PRINT "          R----REVIEW EXISTING DATA FILE"
110 PRINT "          E----END PROGRAM"
120 PRINT "          ?"
130 B$=INKEY$:IF B$="" THEN 130
140 IF B$="A" THEN 180
150 IF B$="R" THEN 380
160 IF B$="E" THEN END
170 PRINT "      PLEASE USE MENU CODE!":BEEP:GOTO 120
180 OPEN "B:CI.DAT" FOR APPEND AS 1
190 CLS
200 INPUT "      PLOT NUMBER AS XXXX (RETURN TO END)";P$
210 IF P$="" THEN CLOSE #1:GOTO10
220 IF LEN(P$)<>4 THEN PRINT"INCORRECT NUMBER LENTH!":BEEP
      :BEEP:GOTO 200
230 IF VAL(MID$(P$,1,1))=3 THEN 290
240 FOR A=1 TO 3
250 P$=MID$(STR$(A),2)+MID$(P$,2,3)
260 GOSUB 340
270 NEXT
280 GOTO 190
290 FOR A=3 TO 1 STEP -1
300 P$=MID$(STR$(A),2)+MID$(P$,2,3)
310 GOSUB 340
320 NEXT
330 GOTO 190
340 INPUT"      CONE INDEX VALUE";AV
350 PRINT
360 PRINT #1,USING "\ \,####";P$,AV
370 RETURN
380 OPEN "B:CI.DAT" FOR INPUT AS 1
390 LPRINT" PLOT NUMBER          CONE INDEX (kPa)"

```

```
400 IF EOF(1) THEN GOTO 450
410 INPUT #1,P$,AV
420 PRINT"  PLOT NUMBER--"P$"  AVERAGE CONE INDEX
      (kPa)="AV"
430 LPRINT"                "P$" "AV
440 GOTO 400
450 LPRINT CHR$(12)
460 FOR X=1 TO 100:NEXT :CLOSE #1
470 GOTO 10
```

APPENDIX G

TIRE TEST AND CONE

INDEX DATA

Plot No.	Static Load	Act. Speed	Wheel Slip	Net Pull	Axle Torque	Cone Index	Aspect Ratio
-	(kN)	(km/h)	(%)	(kN)	(kN-m)	(kPa)	-
11AA	14.46	3.93	59.60	7.170	6.11	345	0.289
21AA	14.28	4.09	55.93	7.708	6.18	563	0.289
31AA	14.44	3.81	58.38	8.064	6.49	809	0.289
12AA	15.19	4.49	47.40	6.761	5.66	300	0.289
22AA	14.97	4.54	42.30	6.886	5.58	544	0.289
32AA	14.76	4.65	45.48	7.019	5.59	721	0.289
13AA	14.96	4.54	48.65	5.524	5.18	409	0.289
23AA	14.52	4.83	40.71	6.797	5.55	477	0.289
33AA	14.56	4.42	43.79	6.672	5.57	582	0.289
14AA	15.17	3.97	59.39	6.174	5.65	495	0.289
24AA	14.53	7.02	27.62	6.930	5.98	658	0.289
34AA	14.77	4.31	53.87	6.957	5.84	647	0.289
15AA	17.66	5.55	0.00	0.925	0.00	482	0.289
25AA	17.85	5.66	0.00	0.467	0.00	647	0.289
35AA	17.67	5.60	0.00	0.729	0.00	609	0.289
11BA	17.41	5.44	15.00	5.040	5.38	500	0.266
21BA	16.80	5.44	22.25	6.427	6.30	606	0.266
31BA	16.95	5.55	18.71	6.192	5.96	835	0.266
12BA	17.58	5.33	12.76	4.172	4.50	293	0.266
22BA	16.81	5.39	19.68	5.778	5.93	371	0.266
32BA	16.35	4.83	17.87	7.046	6.70	673	0.266
13BA	15.52	4.49	14.50	5.720	6.09	374	0.266
23BA	14.83	4.99	31.53	6.632	7.10	442	0.266
33BA	14.91	4.88	25.25	6.298	6.50	628	0.266
14BA	15.89	4.83	36.56	7.135	7.57	474	0.266
24BA	16.28	4.88	32.88	6.988	7.22	682	0.266
34BA	16.13	5.05	27.25	7.619	7.37	624	0.266
15BA	19.82	5.28	0.00	1.401	0.00	427	0.266
25BA	19.66	5.39	0.00	1.477	0.00	462	0.266
35BA	19.73	5.39	0.00	1.121	0.00	399	0.266
11CA	4.37	4.09	46.59	2.055	1.42	337	0.212
21CA	4.87	4.04	47.76	2.411	1.43	462	0.212
31CA	5.28	4.94	34.36	1.094	0.58	719	0.212

APPENDIX G (continued)

Plot No.	Static Load	Act. Speed	Wheel Slip	Net Pull	Axle Torque	Cone Index	Aspect Ratio
-	(kN)	(km/h)	(%)	(kN)	(kN-m)	(kPa)	-
12CA	4.90	4.76	35.66	1.139	0.85	296	0.212
22CA	5.16	5.21	32.71	0.285	0.26	352	0.212
32CA	4.75	4.83	37.95	1.139	0.78	583	0.212
13CA	4.79	4.65	39.99	1.188	0.88	444	0.212
23CA	4.92	4.99	36.01	0.876	0.65	512	0.212
33CA	4.65	4.71	38.41	1.539	1.00	646	0.212
14CA	4.82	4.60	34.43	1.201	0.78	382	0.212
24CA	4.68	4.42	36.24	1.148	0.82	440	0.212
34CA	4.82	4.60	33.40	0.547	0.51	517	0.212
15CA	5.33	5.28	0.00	0.605	0.00	376	0.212
25CA	5.10	5.21	0.00	0.427	0.00	360	0.212
35CA	5.30	5.21	0.00	0.503	0.00	372	0.212
11DA	12.87	4.76	36.48	7.241	5.99	222	0.251
21DA	12.45	4.88	35.94	7.806	6.62	507	0.251
31DA	12.72	4.88	28.72	7.072	5.14	607	0.251
12DA	12.78	4.83	21.59	6.112	5.32	285	0.251
22DA	12.39	4.88	29.34	7.112	6.08	498	0.251
32DA	12.73	4.83	26.12	6.850	5.75	590	0.251
13DA	13.67	4.76	23.14	5.387	5.03	392	0.251
23DA	12.94	5.05	28.59	6.966	5.84	604	0.251
33DA	13.34	5.05	21.65	5.849	4.94	733	0.251
14DA	13.03	4.65	30.16	6.009	5.72	288	0.251
24DA	13.07	4.71	25.99	5.943	5.22	401	0.251
34DA	12.50	4.65	34.54	7.321	6.34	486	0.251
15DA	16.09	5.50	0.00	1.210	0.00	426	0.251
25DA	15.88	5.55	0.00	1.152	0.00	673	0.251
35DA	15.98	5.44	0.00	0.756	0.00	809	0.251
11EA	5.88	5.28	13.45	2.019	1.53	382	0.195
21EA	6.10	5.39	13.18	2.371	1.64	583	0.195
31EA	6.14	5.55	16.10	2.482	1.62	782	0.195
12EA	6.61	4.88	4.79	2.482	1.72	312	0.195
22EA	7.16	5.28	7.36	1.686	1.00	479	0.195
32EA	7.28	5.21	6.54	1.348	0.77	640	0.195
13EA	6.18	4.42	34.53	4.315	3.30	341	0.195
23EA	6.04	4.71	26.64	3.799	2.95	442	0.195
33EA	6.46	4.49	30.13	3.785	2.89	623	0.195
14EA	5.92	4.71	20.40	3.545	2.55	357	0.195
24EA	6.15	5.05	26.61	3.216	2.40	477	0.195
34EA	6.07	4.71	32.88	3.830	2.87	524	0.195
15EA	7.59	5.33	0.00	0.676	0.00	417	0.195
25EA	7.59	5.50	0.00	0.814	0.00	468	0.195
35EA	7.45	5.39	0.00	0.685	0.00	447	0.195
11FA	9.30	5.10	34.42	3.856	3.29	289	0.289
21FA	9.49	4.88	35.48	3.759	3.19	358	0.289

APPENDIX G (continued)

Plot No.	Static Load	Act. Speed	Wheel Slip	Net Pull	Axle Torque	Cone Index	Aspect Ratio
-	(kN)	(km/h)	(%)	(kN)	(kN-m)	(kPa)	-
31FA	9.33	4.31	47.78	4.457	3.56	630	0.289
12FA	8.90	4.54	47.30	3.932	3.38	349	0.289
22FA	8.78	4.20	51.20	3.981	3.57	452	0.289
32FA	8.90	4.76	42.08	3.870	3.30	515	0.289
13FA	9.25	4.54	41.93	3.585	3.11	376	0.289
23FA	9.25	4.88	42.75	3.803	3.17	486	0.289
33FA	9.20	4.42	47.86	4.106	3.51	540	0.289
14FA	8.89	4.60	47.69	3.732	3.26	285	0.289
24FA	8.70	4.71	46.46	3.852	3.30	459	0.289
34FA	8.88	4.76	45.16	3.990	3.29	456	0.289
15FA	10.84	5.33	0.00	0.423	0.00	446	0.289
25FA	10.85	5.50	0.00	0.342	0.00	482	0.289
35FA	10.90	5.44	0.00	0.467	0.00	383	0.289
11GA	11.97	4.31	44.42	4.884	4.21	254	0.289
21GA	11.62	4.54	42.43	5.311	4.42	541	0.289
31GA	11.79	4.49	43.72	5.475	4.54	606	0.289
12GA	11.80	4.76	45.46	5.000	4.30	300	0.289
22GA	11.64	4.65	47.28	5.346	4.58	439	0.289
32GA	11.57	4.71	47.47	5.742	4.65	590	0.289
13GA	12.07	4.83	42.81	4.194	3.67	317	0.289
23GA	11.76	4.71	44.03	5.151	4.31	502	0.289
33GA	11.33	4.49	46.39	5.453	4.65	558	0.289
14GA	12.16	4.26	58.14	4.875	4.36	452	0.289
24GA	12.17	4.88	43.87	4.888	4.18	599	0.289
34GA	11.78	4.49	51.92	5.449	4.65	613	0.289
15GA	14.50	5.66	0.00	0.623	0.00	471	0.289
25GA	14.67	5.66	0.00	0.538	0.00	494	0.289
35GA	14.58	5.66	0.00	0.872	0.00	488	0.289
11HA	17.73	4.65	45.83	7.722	6.50	329	0.289
21HA	17.47	4.76	41.55	8.407	6.49	501	0.289
31HA	18.21	4.83	35.23	7.517	5.86	800	0.289
12HA	17.68	4.65	47.17	7.032	6.33	255	0.289
22HA	17.71	4.94	42.25	7.815	6.40	471	0.289
32HA	17.79	4.88	43.37	7.602	6.33	628	0.289
13HA	18.23	5.28	43.24	6.908	6.19	303	0.289
23HA	17.73	4.71	46.20	8.100	6.65	432	0.289
33HA	17.81	5.05	43.32	7.686	6.22	620	0.289
14HA	18.08	4.76	47.70	7.926	6.45	393	0.289
24HA	17.81	5.82	32.06	8.545	6.80	489	0.289
34HA	17.82	4.71	46.82	8.625	6.76	503	0.289
15HA	21.42	5.71	0.00	1.245	0.00	434	0.289
25HA	21.47	5.71	0.00	0.930	0.00	429	0.289
35HA	21.38	5.71	0.00	1.624	0.00	343	0.289
11AB	14.70	4.49	32.10	5.765	5.13	434	0.289

APPENDIX G (continued)

Plot No.	Static Load	Act. Speed	Wheel Slip	Net Pull	Axle Torque	Cone Index	Aspect Ratio
-	(kN)	(km/h)	(%)	(kN)	(kN-m)	(kPa)	-
21AB	14.94	4.71	25.11	5.898	4.74	575	0.289
31AB	14.50	4.38	30.64	6.761	5.42	785	0.289
22AB	15.35	5.05	36.82	4.866	4.16	493	0.289
32AB	15.26	4.88	30.64	5.418	4.48	760	0.289
23AB	15.68	5.21	34.97	4.190	3.56	481	0.289
33AB	15.63	5.05	31.56	3.825	3.44	635	0.289
14AB	16.43	5.50	42.69	3.501	3.59	270	0.289
24AB	16.87	5.21	30.91	2.611	2.54	413	0.289
15AB	17.97	5.60	0.00	0.725	0.00	320	0.289
25AB	17.86	5.71	0.00	0.547	0.00	515	0.289
35AB	17.95	5.60	0.00	0.863	0.00	424	0.289
11AC	14.69	4.42	52.43	6.169	5.53	296	0.289
21AC	14.40	9.03	-4.68	7.099	5.67	464	0.289
31AC	14.29	4.63	46.94	7.241	5.81	709	0.289
12AC	14.63	9.70	-0.50	6.249	5.45	415	0.289
22AC	14.38	4.83	49.59	6.356	5.39	465	0.289
32AC	14.31	4.99	47.35	6.948	5.71	616	0.289
13AC	14.47	4.71	56.48	6.049	5.44	437	0.289
23AC	14.65	5.05	44.00	5.978	4.95	537	0.289
33AC	14.42	7.51	16.18	6.530	5.43	606	0.289
14AC	15.47	5.39	41.97	3.799	3.47	346	0.289
24AC	14.86	5.21	45.53	5.796	4.83	485	0.289
34AC	14.50	4.83	39.89	5.533	4.83	579	0.289
15AC	17.58	5.60	0.00	0.947	0.00	290	0.289
25AC	17.58	5.71	0.00	0.747	0.00	385	0.289
35AC	17.35	5.55	0.00	1.103	0.00	312	0.289
11AD	14.51	4.20	45.82	6.779	5.66	370	0.289
21AD	14.34	4.42	40.25	7.001	5.64	638	0.289
31AD	14.59	5.39	13.88	6.663	5.23	850	0.289
12AD	14.55	4.31	53.08	6.347	5.58	375	0.289
22AD	14.60	4.38	48.53	7.299	5.83	446	0.289
13AD	14.60	4.20	50.37	5.947	5.42	416	0.289
23AD	14.29	4.42	48.54	6.770	5.74	485	0.289
33AD	14.24	4.54	44.69	7.010	5.72	522	0.289
14AD	14.71	3.97	57.79	6.138	5.80	371	0.289
24AD	14.52	4.26	54.39	7.166	6.08	632	0.289
34AD	14.34	4.71	47.82	7.126	5.94	650	0.289
15AD	17.57	5.50	0.00	0.965	0.00	405	0.289
25AD	17.68	5.60	0.00	0.801	0.00	554	0.289
35AD	17.78	5.44	0.00	0.712	0.00	584	0.289
11AE	14.27	2.57	19.10	6.890	5.60	464	0.289
21AE	14.22	2.57	17.25	6.903	5.57	665	0.289
31AE	14.49	2.64	8.97	6.663	5.31	833	0.289
12AE	14.38	2.19	21.48	0.449	5.50	323	0.289

APPENDIX G (continued)

Plot No.	Static Load	Act. Speed	Wheel Slip	Net Pull	Axle Torque	Cone Index	Aspect Ratio
-	(kN)	(km/h)	(%)	(kN)	(kN-m)	(kPa)	-
22AE	14.13	2.12	16.10	7.135	5.85	458	0.289
32AE	13.81	1.96	23.20	6.961	6.04	516	0.289
13AE	15.71	2.12	2.77	4.719	4.22	368	0.289
23AE	15.89	1.96	-2.05	4.479	3.89	517	0.289
33AE	15.84	1.96	-2.08	4.742	4.00	627	0.289
14AE	15.59	1.96	2.34	5.395	4.90	379	0.289
15AE	17.54	2.19	0.00	1.303	0.00	345	0.289
25AE	17.61	2.30	0.00	0.801	0.00	307	0.289
35AE	17.51	2.12	0.00	1.423	0.00	322	0.289
11AF	14.38	3.20	28.25	6.418	5.40	366	0.289
21AF	14.11	2.75	41.14	7.633	6.15	504	0.289
31AF	14.06	2.91	27.60	7.664	6.26	786	0.289
32AF	14.02	3.14	37.20	7.210	6.03	774	0.289
13AF	15.00	3.25	38.00	6.316	5.57	321	0.289
33AF	14.63	3.31	31.90	6.961	5.95	594	0.289
14AF	15.33	3.31	25.33	5.991	5.28	327	0.289
24AF	15.19	3.36	22.12	6.152	5.08	603	0.289
15AF	17.86	3.93	0.00	0.560	0.00	387	0.289
25AF	17.83	3.97	0.00	0.636	0.00	521	0.289
35AF	17.83	4.04	0.00	0.681	0.00	474	0.289
11AG	14.28	6.73	60.37	6.854	5.58	622	0.289
21AG	14.52	6.90	59.79	6.730	5.53	704	0.289
22AG	14.63	5.71	65.33	7.255	6.11	661	0.289
13AG	14.86	6.34	61.83	6.063	5.32	388	0.289
14AG	15.44	7.13	55.73	5.133	4.65	286	0.289
34AG	14.72	7.29	54.86	5.725	5.00	574	0.289
15AG	17.68	7.85	0.00	1.036	0.00	451	0.289
25AG	17.81	8.01	0.00	0.445	0.00	599	0.289
35AG	18.05	7.85	0.00	0.738	0.00	625	0.289

APPENDIX H

π TERM GENERATION PROGRAM

```

10  DIM P$(210),W(210),SP(210),SL(210),P(210),T(210),
      VL(210),CI(210),PR(210),B(210),D(210)
20  OPEN "B:TTCI.DAT" FOR INPUT AS #1
30  FOR X=1 TO 194
40    INPUT #1,P$(X),W(X),SP(X),SL(X),P(X),T(X),VL(X),
          CI(X),RR(X),B(X),D(X))
41    PRINT P$(X)
45    IF EOF(1) THEN 60
50    NEXT X
60  CLOSE #1
70  OPEN "B:PITERM.DAT" FOR OUTPUT AS #1
80  FOR X=1 TO 194
90    PI1=P(X)/(W(X)-VL(X))           :REM PULL TO LOAD
                                       RATIO
100   PI2=CI(X)*.145*B(X)*D(X)/(W(X)-VL(X))
                                       :REM WHEEL NUMERIC
110   PI3=SL(X)                       :REM WHEEL SLIP
120   PI4B=(SP(X)*(5280/3600))^2/(32.2*B(X)/12)
                                       :REM VELOCITY
                                       COEFFICIENT
125   PI4D=(SP(X)*(5280/3600))^2/(32.2*D(X)/12)
                                       :REM VELOCITY
                                       COEFFICIENT
130   PI5=B(X)/D(X)                   :REM ASPECT RATIO
140   PRINT USING "\ \, #.#####   .#####   .#####   #.#####
      ##.#####^ ^ ^ ^ ##.##^ ^ ^ ^ .#####";P$(X),PI1,PI2,PI3,
      PI4B,PI4D,PI5
145   LPRINT USING "\ \, #.#####   .#####   .#####   #.#####
      ##.#####^ ^ ^ ^ ##.##^ ^ ^ ^ .#####";P$(X),PI1,PI2,PI3,
      PI4B,PI4D,PI5
150   PRINT #1,USING "\ \, #.#####   .#####   .#####   #.#####
      ##.#####^ ^ ^ ^ ##.##^ ^ ^ ^ .#####";P$(X),PI1,PI2,PI3,
      PI4B ,PI4D,PI5
160  NEXT
170  CLOSE #1

```

APPENDIX I

TERM DATA

Plot	π_1	π_2	π_3	π_4	π_5
11AA	0.496	15.21	0.498	1.120E+00	0.2889
21AA	0.540	25.13	0.453	1.024E+00	0.2889
31AA	0.558	35.72	0.483	9.962E-01	0.2889
12AA	0.445	12.60	0.347	8.634E-01	0.2889
22AA	0.460	23.18	0.283	7.353E-01	0.2889
32AA	0.475	31.14	0.323	8.649E-01	0.2889
13AA	0.369	17.43	0.362	9.288E-01	0.2889
23AA	0.468	20.94	0.263	7.849E-01	0.2889
33AA	0.458	25.48	0.302	7.372E-01	0.2889
14AA	0.407	20.81	0.495	1.140E+00	0.2889
24AA	0.477	28.87	0.101	1.113E+00	0.2889
34AA	0.471	27.94	0.427	1.039E+00	0.2889
11BA	0.290	23.56	-0.056	4.464E-01	0.2663
21BA	0.383	29.58	0.034	5.332E-01	0.2663
31BA	0.365	40.39	-0.010	5.085E-01	0.2663
12BA	0.237	13.66	-0.084	4.064E-01	0.2663
22BA	0.344	18.10	0.002	4.898E-01	0.2663
32BA	0.431	33.76	-0.020	3.758E-01	0.2663
13BA	0.368	19.76	-0.062	2.999E-01	0.2663
23BA	0.447	24.45	0.149	5.790E-01	0.2663
33BA	0.423	34.55	0.071	4.643E-01	0.2663
14BA	0.449	24.46	0.212	6.298E-01	0.2663
24BA	0.429	34.36	0.203	6.298E-01	0.2663
34BA	0.472	31.73	0.175	6.298E-01	0.2663
11CA	0.470	16.13	0.336	1.419E+00	0.2123
21CA	0.495	19.87	0.351	1.443E+00	0.2123
31CA	0.207	28.48	0.185	1.366E+00	0.2123
12CA	0.232	12.64	0.201	1.326E+00	0.2123
22CA	0.055	14.28	0.164	1.451E+00	0.2123
32CA	0.239	25.66	0.229	1.460E+00	0.2123
13CA	0.248	19.38	0.255	1.454E+00	0.2123
23CA	0.178	21.76	0.205	1.470E+00	0.2123
33CA	0.331	29.09	0.235	1.413E+00	0.2123
14CA	0.249	16.58	0.185	1.188E+00	0.2123
24CA	0.245	19.68	0.208	1.166E+00	0.2123
34CA	0.114	22.46	0.173	1.152E+00	0.2123
11DA	0.563	10.65	0.211	7.287E-01	0.2508
21DA	0.627	25.16	0.204	7.504E-01	0.2508

APPENDIX I (continued)

Plot	π_1	π_2	π_3	π_4	π_5
31DA	0.556	29.49	0.115	6.062E-01	0.2508
12DA	0.478	13.77	0.026	4.897E-01	0.2508
22DA	0.574	24.83	0.122	6.166E-01	0.2508
32DA	0.538	28.63	0.083	5.515E-01	0.2508
13DA	0.394	17.71	0.045	4.976E-01	0.2508
23DA	0.538	28.84	0.113	6.461E-01	0.2508
33DA	0.438	33.95	0.027	5.371E-01	0.2508
14DA	0.461	13.66	0.132	5.747E-01	0.2508
24DA	0.455	18.96	0.081	5.242E-01	0.2508
34DA	0.586	24.02	0.187	6.543E-01	0.2508
11EA	0.344	26.96	-.075	6.644E-01	0.1951
21EA	0.389	39.64	-.079	6.885E-01	0.1951
31EA	0.404	52.82	-.042	7.843E-01	0.1951
12EA	0.375	19.56	-.182	4.703E-01	0.1951
22EA	0.236	27.75	-.151	5.797E-01	0.1951
32EA	0.185	36.44	-.161	5.576E-01	0.1951
13EA	0.698	22.87	0.186	8.196E-01	0.1951
23EA	0.629	30.34	0.088	7.380E-01	0.1951
33EA	0.586	40.00	0.132	7.380E-01	0.1951
14EA	0.598	24.98	0.011	6.273E-01	0.1951
24EA	0.523	32.17	0.088	8.470E-01	0.1951
34EA	0.631	35.81	0.166	8.818E-01	0.1951
11FA	0.415	12.88	0.185	1.084E+00	0.1951
21FA	0.396	15.64	0.199	1.024E+00	0.1951
31FA	0.478	28.01	0.351	1.224E+00	0.1951
12FA	0.442	16.25	0.345	1.330E+00	0.1951
22FA	0.453	21.34	0.394	1.330E+00	0.1951
32FA	0.435	23.99	0.280	1.213E+00	0.1951
13FA	0.388	16.85	0.279	1.096E+00	0.1951
23FA	0.411	21.78	0.289	1.300E+00	0.1951
33FA	0.446	24.33	0.352	1.293E+00	0.1951
14FA	0.420	13.29	0.350	1.383E+00	0.1951
24FA	0.443	21.87	0.335	1.386E+00	0.1951
34FA	0.449	21.29	0.319	1.353E+00	0.1951
11GA	0.408	8.80	0.309	1.081E+00	0.1951
21GA	0.457	19.31	0.308	1.190E+00	0.1951
31GA	0.465	21.32	0.301	1.138E+00	0.1951
12GA	0.424	10.54	0.322	1.368E+00	0.1951
22GA	0.459	15.64	0.345	1.396E+00	0.1951
32GA	0.496	21.14	0.347	1.440E+00	0.1951
13GA	0.348	10.89	0.290	1.274E+00	0.1951
23GA	0.438	17.69	0.305	1.269E+00	0.1951
33GA	0.481	20.41	0.334	1.254E+00	0.1951
14GA	0.401	15.42	0.480	1.856E+00	0.1951
24GA	0.402	20.42	0.303	1.353E+00	0.1951
34GA	0.462	21.57	0.403	1.559E+00	0.1951
11HA	0.435	7.69	0.327	1.322E+00	0.1951

APPENDIX I (continued)

Plot	π_1	π_2	π_3	π_4	π_5
21HA	0.481	11.89	0.274	1.191E+00	0.1951
31HA	0.413	18.22	0.196	9.929E-01	0.1951
12HA	0.398	5.98	0.344	1.390E+00	0.1951
22HA	0.441	11.03	0.283	1.308E+00	0.1951
32HA	0.427	14.64	0.297	1.329E+00	0.1951
13HA	0.379	6.89	0.295	1.544E+00	0.1951
23HA	0.457	10.10	0.332	1.373E+00	0.1951
33HA	0.432	14.43	0.296	1.420E+00	0.1951
14HA	0.438	9.01	0.350	1.487E+00	0.1951
24HA	0.480	11.38	0.156	1.320E+00	0.1951
34HA	0.484	11.70	0.339	1.405E+00	0.1951
11AB	0.392	12.24	0.157	7.815E-01	0.1951
21AB	0.395	15.96	0.069	7.082E-01	0.1951
31AB	0.466	22.45	0.138	7.123E-01	0.1951
22AB	0.317	13.31	0.214	1.139E+00	0.1951
32AB	0.355	20.65	0.139	8.860E-01	0.1951
23AB	0.267	12.72	0.193	1.152E+00	0.1951
33AB	0.245	16.84	0.150	9.739E-01	0.1951
14AB	0.213	6.81	0.288	1.647E+00	0.1951
24AB	0.155	10.15	0.142	1.020E+00	0.1951
11AC	0.420	8.36	0.409	1.553E+00	0.1951
31AC	0.507	20.58	0.327	1.312E+00	0.1951
22AC	0.442	13.40	0.374	1.639E+00	0.1951
32AC	0.485	17.84	0.346	1.609E+00	0.1951
13AC	0.418	12.52	0.459	2.098E+00	0.1951
23AC	0.408	15.20	0.304	1.454E+00	0.1951
33AC	0.453	17.43	-0.041	1.439E+00	0.1951
14AC	0.246	9.28	0.273	1.517E+00	0.1951
24AC	0.390	13.53	0.323	1.641E+00	0.1951
34AC	0.381	16.55	0.253	1.152E+00	0.1951
11AD	0.467	10.57	0.327	1.079E+00	0.1951
21AD	0.488	18.44	0.258	9.840E-01	0.1951
31AD	0.457	24.16	-0.070	6.996E-01	0.1951
12AD	0.436	10.68	0.417	1.517E+00	0.1951
22AD	0.500	12.67	0.361	1.293E+00	0.1951
13AD	0.407	11.82	0.383	1.286E+00	0.1951
23AD	0.474	14.07	0.361	1.327E+00	0.1951
33AD	0.492	15.20	0.313	1.208E+00	0.1951
14AD	0.417	10.46	0.476	1.593E+00	0.1951
24AD	0.494	18.05	0.433	1.563E+00	0.1951
34AD	0.497	18.80	0.352	1.460E+00	0.1951
11AE	0.483	13.48	0.191	2.810E-01	0.1951
21AE	0.486	19.40	0.173	2.686E-01	0.1951
31AE	0.460	23.83	0.090	2.318E-01	0.1951
12AE	0.031	9.31	0.215	2.144E-01	0.1951
22AE	0.505	13.44	0.161	1.782E-01	0.1951
32AE	0.504	15.50	0.232	1.803E-01	0.1951

APPENDIX I (continued)

Plot	π_1	π_2	π_3	π_4	π_5
13AE	0.300	9.71	0.028	1.327E-01	0.1951
14AE	0.346	10.08	0.023	1.115E-01	0.1951
11AF	0.446	10.55	0.109	3.555E-01	0.1951
21AF	0.541	14.81	0.269	3.902E-01	0.1951
31AF	0.545	23.19	0.276	4.483E-01	0.1951
32AF	0.514	22.89	0.220	4.478E-01	0.1951
13AF	0.421	8.87	0.230	4.929E-01	0.1951
33AF	0.476	16.84	0.154	4.225E-01	0.1951
14AF	0.391	8.85	0.072	3.514E-01	0.1951
24AF	0.405	16.45	0.221	5.159E-01	0.1951
11AG	0.480	18.06	0.508	5.163E+00	0.1951
21AG	0.464	20.11	0.500	5.269E+00	0.1951
22AG	0.496	18.74	0.569	4.873E+00	0.1951
13AG	0.408	10.83	0.526	4.935E+00	0.1951
14AG	0.332	7.68	0.450	4.634E+00	0.1951
34AG	0.389	16.17	0.439	4.670E+00	0.1951

APPENDIX J

DATA FOR VALIDATION OF
PREDICTION EQUATION

π_1	π_2	π_3	π_4	π_5
0.290	34.555	0.3336	1.017E-02	0.4125
0.437	28.589	0.6672	1.324E-02	0.4125
0.319	16.657	0.3161	1.377E-02	0.4125
0.506	33.109	0.5426	1.295E-02	0.4125
0.470	10.850	0.5036	4.582E-03	0.4125
0.261	10.822	0.2662	6.204E-03	0.4125
0.340	17.631	0.3494	7.379E-03	0.4125
0.504	8.495	0.4342	6.204E-03	0.4125
0.412	10.477	0.3575	7.379E-03	0.4125
0.266	14.909	0.2451	1.734E-02	0.4125
0.520	7.727	0.3862	1.557E-02	0.4125
0.363	8.122	0.3765	9.121E-03	0.4125
0.419	23.419	0.3585	1.355E-02	0.4125
0.307	6.725	0.3331	1.374E-02	0.4125
0.338	12.178	0.2781	1.471E-02	0.4125
0.436	13.677	0.3368	1.764E-02	0.4125
0.262	5.597	0.2293	1.385E-02	0.4125
0.186	6.741	0.2621	1.425E-02	0.4125
0.091	9.876	0.2245	1.311E-02	0.4125
0.281	5.625	0.2539	1.501E-02	0.4125
0.274	9.853	0.2545	1.747E-02	0.4125
0.338	10.658	0.2891	1.888E-02	0.4125
0.202	4.645	0.2679	1.408E-02	0.4125
0.227	7.894	0.3236	1.324E-02	0.4125

VITA

Joseph Garland Greenlee

Candidate for the Degree of

Master of Science

Thesis: EFFECT OF VELOCITY ON TRACTIVE PERFORMANCE OF
TRACTOR TIRES.

Major Field: Agricultural Engineering

Biographical:

Personal Data: Born in Oklahoma City, Oklahoma, June
20, 1961, the son of Joe E. and Norma Greenlee.
married to Tonya A. Leach on August 1, 1981.

Education: Graduated from Holdenville High School,
Holdenville, Oklahoma, in May, 1979; received
Bachelor of Science Degree in Agricultural
Engineering from Oklahoma State University in
May, 1985; completed requirements for Master of
Science Degree at Oklahoma State University in
December, 1986.

Professional Experience: Research Assistant, Depart-
ment of Agricultural Engineering, Oklahoma
State University, June 1985 to December 1986.